N.A.E

R. & M. No. 2733
(13,323)
A.R.C. Technical Report

MINISTRY OF SUPPLY

AERONAUTICAL RESEARCH COUNCIL
REPORTS AND MEMORANDA

20 OCT 1954

Helicopter Control to Trim in Forward Flight

By

W. STEWART, B.Sc.

NATIONAL AERONAUTICAL ESTABLISHMENT
Library
20 OCT 1954
LIBRARY
NATIONAL AERONAUTICAL ESTABLISHMENT

Crown Copyright Reserved

LONDON: HER MAJESTY'S STATIONERY OFFICE
1954
NINE SHILLINGS NET

Helicopter Control to Trim in Forward Flight

By

W. STEWART, B.Sc.

COMMUNICATED BY THE PRINCIPAL DIRECTOR OF SCIENTIFIC RESEARCH (AIR), MINISTRY OF SUPPLY

*Reports and Memoranda No. 2733**

March, 1950

Royal Aircraft Establishment
20 OCT 1954
LIBRARY

Summary.—A theoretical estimation of the flapping and feathering (cyclic pitch) to trim the helicopter rotor in forward flight is given and the equivalence of the two systems is shown.

The feathering amplitudes to trim the complete helicopter are then estimated and compared with experimental flight values obtained on the Sikorsky R–4B and S–51 helicopters. The effects of centre of gravity position, fuselage pitching moment, etc., are considered and the delta-3 hinge effect is dealt with in an appendix. The effect of slipstream curvature on lateral control is included.

Satisfactory agreement of the theoretical and experimental results is obtained. In the longitudinal trim, the fuselage pitching moment in the presence of the rotor slipstream is a most important contribution. In the lateral trim, the induced velocity distribution and the tail rotor behaviour have a large influence and must be taken into account.

1. *Introduction.*—For a single-rotor helicopter with hinged blades and in steady rectilinear flight, there is a variation in the resultant air velocity at the blade as the latter rotates in azimuth. To counteract the velocity changes and so to trim the helicopter rotor an appropriate flapping and/or feathering (cyclic pitch) of the blades is required. For most of the present-day helicopters, feathering control is used and the present report gives a theoretical analysis of the feathering amplitudes required to trim the helicopter. Nevertheless, the flapping and feathering methods of rotor control are very similar aerodynamically and the equivalence of the two systems is shown in detail in this report.

There has always been some ambiguity in the definitions of the thrust, flow through the disc, flapping and feathering coefficients, etc., when flapping and feathering systems are discussed. It is therefore necessary, without bringing anything new into helicopter theory, to establish some basic definitions required for the study of blade motion, particularly in showing the relationship of the pure flapping and pure feathering systems. The following definitions are used throughout this report.

Geometric flapping angle is the angle between the longitudinal blade axis and a plane perpendicular to the rotor shaft. Due to possible blade bending it is difficult to define the direction of the blade longitudinal axis and in this report it is assumed that the blade remains straight in

* R.A.E. Report Aero. 2358, received 25th August, 1950.

the theoretical analysis while for the experimental work, as in Ref. 3, the blade axis is the line joining the blade root and the 0·75-radius position. The geometric flapping angle may be expressed by

$$\beta_s = a_{0s} - a_{1s} \cos \psi - b_{1s} \sin \psi - a_{2s} \cos 2\psi - b_{2s} \sin 2\psi - \ldots . \quad (1)$$

where ψ is the azimuth position of the blade measured from the downwind position in the direction of rotation.

a_{0s} is the coning angle of the blades.

a_{1s} is the amplitude of flapping equal to the longitudinal tilt of the rotor disc plane, backwards for a positive value of a_{1s}.

b_{1s} is the lateral tilt of the rotor disc plane due to the flapping, a positive value of b_{1s} giving a tilt of the disc towards the advancing blade ($\psi = 90$ deg).

Flapping angle of the blade (or the aerodynamic flapping angle due to the velocity variations in forward flight) is the angle between the blade axis and the plane of no-feathering and is defined by

$$\beta = a_0 - a_1 \cos \psi - b_1 \sin \psi - a_2 \cos 2\psi - b_2 \sin 2\psi - \ldots . \quad (2)$$

where the amplitudes have the same interpretation as above except that they are referred to the no-feathering axis.

Blade pitch angle is the angle between the no-lift chord of the blade section and the plane perpendicular to the rotor shaft and is given by

$$\vartheta = \vartheta_0 - A_1 \cos \psi - B_1 \sin \psi - A_2 \cos 2\psi - B_2 \sin 2\psi - \ldots . \quad (3)$$

where ϑ_0 is called the collective pitch of the blades.

B_1 is the feathering amplitude equal to the longitudinal tilt of the no-feathering axis, positive values of B_1 giving a forward tilt.

A_1 is the feathering amplitude equal to the lateral tilt of the no-feathering axis, positive values of A_1 giving a tilt towards the advancing blade.

A further simplified explanation of the no-feathering axis conception may be useful. Let us assume a rotor with flapping blades and without any feathering applied to it ; for simplicity the blade chord may be taken parallel to the flapping hinge. Now let us tilt the rotor *disc* forward by an angle i_D from the plane perpendicular to the shaft, *i.e.*, without tilting the shaft. Due to the fact that the flapping hinges are rigidly connected to the rotor shaft, the relative tilt will produce a feathering in the plane of the rotor disc in the form

$$i_D \sin \psi .$$

Alternatively, the blades will have a flapping motion relative to the shaft in the form

$$i_D \cos \psi .$$

If the blades of the rotor have already an applied feathering say, $- B_1 \sin \psi$, the resultant feathering will be $(i_D - B_1) \sin \psi$.

It can be seen that by tilting the rotor disc with respect to the plane perpendicular to the rotor shaft by an angle $i_D = B_1$, the feathering in this rotor disc plane would be zero. Such a plane is called the no-feathering plane and its axis is the no-feathering axis. A more detailed discussion of the interchangeability of flapping and feathering axes is given in Ref. 3.

2. *Theory.*—The helicopter is flying with constant velocity V along a straight path inclined at an angle τ to the horizon. The forces acting on the helicopter are as follows :—

(*a*) The rotor forces. These are transmitted to the shaft in the form of a thrust T defined as the force perpendicular to the rotor disc and the force H defined as parallel to the rotor disc.

(*b*) The resultant air force on the helicopter less rotor.

(*c*) The aerodynamic moment of the helicopter less rotor.

(*d*) The weight of the helicopter.

It should be noted that in (*b*) and (*c*) the effect of the rotor slipstream on the fuselage must be included.

As it is assumed that the rotor has hinged blades, the thrust and H-force act at the point of intersection of the rotor axis and the plane perpendicular to the rotor axis passing through the flapping hinges. For a rotor with offset flapping hinges, $e \neq 0$, the rotor transmits a moment proportional to the relative tilt of the rotor and shaft axes. For the more usual case of zero hinge offset, $e = 0$, no moment can be transmitted from the rotor to the shaft.

In steady trimmed flight of the helicopter, the rotor forces must be in equilibrium with the other forces acting on the helicopter, fixing in this way the position of the rotor disc in relation to the flight path.

We will use, after Squire (R. & M. 1730[1]), the system of axes connected with the rotor disc, *i.e.*, thrust axis and rotor axis perpendicular to the rotor disc plane and the H-force axis parallel to the plane of the rotor disc and passing through the apex of the rotor cone, positive in the backward direction.

The diagram of the rotor is shown in Fig. 1. It is assumed that the blades do not bend and are therefore moving along the surface of a cone. For straight blades the tip-path plane is equivalent to the rotor-disc plane. The tip-path plane makes an angle i with the undisturbed stream velocity ; i is an effective angle of attack of the rotor and is positive for helicopter conditions. It is worth pointing out that no reference is made to the rotor shaft and the analysis is made independent of the rotor shaft position with respect to the rotor disc. Assuming that the blades have such a feathering with respect to the tip-path plane that they move along the surface of the above mentioned cone, the present analysis determines the feathering amplitudes to maintain these equilibrium conditions.

The small deviations of the blades from the cone surface are functions of the higher harmonics of flapping 2ψ, 3ψ, etc., and have no effect on the trimmed position of the rotor disc or on the feathering of the fundamental modes. These higher harmonics are the source of vibration in the helicopter and are not within the scope of the present report.

From Fig. 1, the velocity parallel to the tip-path plane is

$$\mu \Omega R$$

and the velocity perpendicular to the tip-path plane is

$$\lambda \Omega R .$$

At the present stage of the theory, it is assumed after Glauert (R. & M. 1111[9]), Lock (R. & M. 1127[2]) and Squire (R. & M. 1730[1]), etc., that λ is constant over the rotor disc.

Let us assume that the instantaneous blade pitch angle measured from the rotor disc plane is given by

$$\vartheta = \vartheta_0 - A_{1D} \cos \psi - B_{1D} \sin \psi . \qquad \ldots \ldots \ldots \ldots \ldots \ldots \ldots \quad (4)$$

This is similar to the definition of equation (3), suffix D being used to denote reference to the disc plane whereas the symbols of equation (3) are referred to the rotor shaft and so far no mention of the rotor shaft is made in the theory.

The coefficients ϑ_0, A_{1D} and B_{1D} are chosen in such a way that the rotor gives the required thrust and the rotor disc maintains its appropriate position in space.

Assuming that the coning angle a_0 is small and that sin a_0 can be replaced by a_0 and cos a_0 by unity, the velocities of the air with respect to a blade element distant $r = xR$ from the rotor axis are as follows.

Velocity tangential to the cone surface and perpendicular to the blade (chordwise) is

$$(x + \mu \sin \psi)\Omega R \quad . . \quad . . \quad . . \quad . . \quad . . \quad . . \quad . . \quad (5)$$

Velocity perpendicular to the blade and to the cone surface (through the disc) is

$$(a_0\mu \cos \psi + \lambda)\Omega R \quad . . \quad . . \quad . . \quad . . \quad . . \quad . . \quad (6)$$

Velocity along the blade (spanwise) is

$$(\mu \cos \psi + \lambda a_0)\Omega R \quad . . \quad . . \quad . . \quad . . \quad . . \quad . . \quad (7)$$

The effect of the spanwise component of the flow is not known. Probably it will thicken the boundary layer, increase the drag and decrease the lift slope of the blade aerofoil section. In the analysis the spanwise component of the flow is neglected but it must be remembered that its effect can be retained empirically in the use of the appropriate values of lift slope and profile-drag coefficient.

Experimental values of thrust and torque coefficients of the rotor show that the value of the lift slope for rotating blades is below the corresponding value for similar aerofoils under rectilinear flow conditions. Myers in his work[3] (1947) was using a value of the lift slope of 5·73; investigations by Brotherhood (R. & M. 2521[13] 1947) show good agreement between rotor theory and flight experiment for a value of 5·6; in the latest N.A.C.A. publications[11,12] (1948) the value is lowered to 5·56. Recent wind-tunnel tests at the Royal Aircraft Establishment seem to indicate an even lower value but this is probably due to scale effect with the low Reynolds number of the model.

The profile-drag coefficient of the rotor blades is larger than that obtained from two-dimensional tunnel tests. Numerical values for blade profile drag can be found in Ref. 3, 11 and 12.

From equations (5) and (6) the effective incidence of the blade element is

$$\alpha = \vartheta_0 - A_{1D} \cos \psi - B_{1D} \sin \psi - \frac{a_0\mu \cos \psi + \lambda}{x + \mu \sin \psi} \quad . . \quad . . \quad . . \quad . . \quad . . \quad (8)$$

and the aerodynamic force acting on the blade element $cR\,dx$ is

$$dF = \tfrac{1}{2}\rho ac\Omega^2R^3(x + \mu \sin \psi)^2\left(\vartheta_0 - A_{1D} \cos \psi - B_{1D} \sin \psi - \frac{a_0\mu \cos \psi + \lambda}{x + \mu \sin \psi}\right)dx \, . \quad . . \quad (9)$$

The corresponding moment with respect to the flapping hinge, assuming that the angle of the flapping hinge axis to the tip-path plane is small

$$dM = xR\,dF$$

$$= \tfrac{1}{2}\rho ac\Omega^2R^4(x + \mu \sin \psi)^2\left(\vartheta_0 - A_{1D} \cos \psi - B_{1D} \sin \psi - \frac{a_0\mu \cos \psi + \lambda}{x + \mu \sin \psi}\right)x\,dx \, . \quad . . \quad (10)$$

Since the angles between resultant airflow and tip-path plane are small the increment of aerodynamic force acting on the blade element can be taken as the thrust increment

$$dF = dT \, . \quad . . \quad . . \quad . . \quad . . \quad . . \quad . . \quad . . \quad . . \quad . . \quad . . \quad (11)$$

It is now further assumed that the blade collective pitch ϑ_0 and the blade chord c are constant along the blade, but the analysis could easily be extended to cover any blade shape and twist, as long as the blade angle and the chord can be expressed as functions of the radius.

Integrating equation (9) between $x = 0$ and 1 we obtain an equation, whose constant term gives the mean value of the rotor thrust. If the integration is carried out between limits other than 0 and 1 the effect of root and tip losses can be taken into account.

Expressing the solution of equation (9) in the form of a thrust coefficient

$$t_c = \frac{T}{bcR\rho\Omega^2R^2}$$

$$= \frac{a}{4}\left[\tfrac{2}{3}\vartheta_0 \frac{1 - \mu^2 + \frac{9}{4}\mu^4}{1 + \frac{3}{2}\mu^2} - \lambda \frac{1 - \frac{1}{2}\mu^2}{1 + \frac{3}{2}\mu^2} \right] . \quad .. \quad .. \quad .. \quad .. \quad .. \quad .. \quad (12)$$

The integration of equation (10) gives the expression for the aerodynamic moment about the flapping hinge. Since the rotor disc is maintained in position, the moments of the air forces and of the centrifugal force about the flapping hinge are in equilibrium: the small effect of the blade weight may be neglected. Thus, to produce no flapping motion relative to the disc-plane position, the solution of equation (10) must be such that the constant term equals the centrifugal force moment and the periodic terms, *i.e.*, coefficients of sin ψ and cos ψ, are zero.

Equating the constant term and the centrifugal force moment gives the coning angle

$$a_0 = \tfrac{1}{2}\gamma_0\left(\tfrac{1}{4}\vartheta_0 \frac{1 - \frac{1}{18}\mu^2 + \frac{3}{2}\mu^4}{1 + \frac{3}{2}\mu^2} - \tfrac{1}{3}\lambda \frac{1 - \frac{1}{2}\mu^2}{1 + \frac{3}{2}\mu^2} \right) \quad .. \quad .. \quad .. \quad (13)$$

where γ_0 is called Lock's Inertia Number and is given by

$$\gamma_0 = \frac{\rho a \bar{c} R^4}{I_1} . \quad .. \quad .. \quad .. \quad .. \quad .. \quad .. \quad .. \quad .. \quad (14)$$

Equating the coefficients of sin ψ and cos ψ to zero, we obtain the feathering amplitudes to trim

$$B_{1D} = 2\mu \frac{\frac{4}{3}\vartheta_0 - \lambda}{1 + \frac{3}{2}\mu^2} \quad .. \quad .. \quad .. \quad .. \quad .. \quad .. \quad .. \quad (15)$$

and

$$A_{1D} = \frac{4}{3}\frac{a_0\mu}{1 + \frac{1}{2}\mu^2} . \quad .. \quad .. \quad .. \quad .. \quad .. \quad .. \quad .. \quad (16)$$

The above method of analysis is similar to that used by Squire and in his work can be found expressions for thrust, H-force and torque coefficients. The equation (12) of the present report is identical with equation (11), and equation (15) is identical with equation (14) of R. & M. 1730[1].

It will be noted that the A_{1D} of equation (16) is proportional to coning angle. In R. & M. 1730[1] and other reports where coning angle is not taken into account no value for this feathering coefficient can be obtained.

3. *Flapping and Feathering.*—The required blade feathering to maintain equilibrium of the rotor disc, as calculated in the previous section and given by equations (15) and (16), can be achieved by two independent methods in practical application to helicopter control.

In one method, the rotor shaft remains perpendicular to the tip-path plane and the required feathering distribution is obtained by rotating the blade about its longitudinal axis (cyclic pitch change) by some mechanical means, *e.g.*, by a suitably tilted swash-plate and system of connecting

links. This method of trimming the rotor disc plane at a given position in the air is called *pure feathering*. By definition of the feathering angles, equation (3), and remembering that in the pure feathering system, the rotor shaft remains perpendicular to the rotor disc,

$$A_{1D} = A_1 \quad .. \quad .. \quad .. \quad .. \quad .. \quad .. \quad .. \quad .. \quad (17)$$

and

$$B_{1D} = B_1 . \quad .. \quad .. \quad .. \quad .. \quad .. \quad .. \quad .. \quad .. \quad (18)$$

The other way of obtaining the required feathering in the rotor disc plane is by tilting the rotor shaft (or hub) with respect to the axis of the tip-path plane. Assume that the rotor shaft (or hub) is tilted forward with respect to the rotor disc axis by an angle a_1 and laterally by an angle b_1. Since the flapping hinge is connected to the hub and since the hub is tilted with respect to the rotor disc plane, the hinge axis changes its setting with respect to this rotor disc plane as the rotor rotates.

Taking for simplicity the case of the longitudinal tilt a_1 alone and with the flapping hinge axis perpendicular to the rotor shaft and to the longitudinal axis of the blade, and assuming no collective pitch $\vartheta_0 = 0$, the following conditions exist. The rotor shaft is tilted forward by an angle a_1. When the blade is in its rearmost position ($\psi = 0$) the hinge axis is parallel with the rotor disc plane and the hinge setting and blade pitch are zero. When the blade has rotated in azimuth to the lateral position ($\psi = 90$ deg) the hinge setting and blade pitch with respect to the rotor disc plane are $- a_1$. As the blade reaches the forward position ($\psi = 180$ deg) the hinge axis is again parallel to the disc plane and the pitch angle is zero. In the $\psi = 270$ deg position, the hinge setting and pitch angle are $+ a_1$. Thus the tilt of the ro tor shaft with respect to the rotor disc plane produces equivalent blade feathering in this plane.

In the general case, where the shaft is tilted forward by an angle a_1 and laterally by an angle b_1, feathering is produced in the plane of the rotor disc in the form

$$- a_1 \sin \psi + b_1 \cos \psi .$$

Comparing this with the expressions for feathering in equation (4) it can be seen that the angles of tilt of the rotor shaft with respect to the rotor disc axis are given by

$$a_1 = B_{1D} \quad .. \quad .. \quad .. \quad .. \quad .. \quad .. \quad .. \quad .. \quad (19)$$

and

$$b_1 = - A_{1D} \quad .. \quad .. \quad .. \quad .. \quad .. \quad .. \quad .. \quad .. \quad (20)$$

where the values of B_{1D} and A_{1D} have been evaluated in equations (15) and (16).

This method of trimming the rotor disc by tilting the shaft (or hub) is called the *pure flapping* system. Transferring the axes of reference from the rotor disc to the rotor shaft, the pure flapping system has now no feathering but the rotor disc is tilted backwards and sideways by angles a_1 and b_1 respectively, which can be expressed as the pure flapping of equation (2), *viz.*,

$$\beta = a_0 - a_1 \cos \psi - b_1 \sin \psi . \quad .. \quad .. \quad .. \quad .. \quad .. \quad (2)$$

Comparing equations (19) with (18) and (20) with (17) it can be said that pure flapping and pure feathering are equivalent when

$$a_1 = B_1 \quad .. \quad .. \quad .. \quad .. \quad .. \quad .. \quad .. \quad .. \quad (21)$$

and

$$b_1 = - A_1 . \quad .. \quad .. \quad .. \quad .. \quad .. \quad .. \quad .. \quad .. \quad (22)$$

In the pure flapping system (tilting hub) there is no feathering with respect to the hub axis which is itself the axis of no-feathering. Due to the forward velocity and to the flapping freedom of the blades the rotor disc tilts from the no-feathering plane into such a position that the acquired

feathering in the rotor disc plane is as given by equations (15) and (16). Hence, the flapping amplitudes equivalent to the tilt of the rotor disc are given by equations (15) and (16) and may be rewritten as

$$a_1 = 2\mu \frac{\frac{4}{3}\vartheta_0 - \lambda}{1 + \frac{3}{2}\mu^2} \quad .. \quad .. \quad .. \quad .. \quad .. \quad .. \quad .. \quad (23)$$

and

$$b_1 = \frac{\frac{4}{3}a_0\mu}{1 + \frac{1}{2}\mu^2} \quad .. \quad .. \quad .. \quad .. \quad .. \quad .. \quad .. \quad (24)$$

where μ and λ are the velocity coefficients with respect to the rotor disc plane (tip-path plane).

The full mathematical treatment of the rotor with flapping blades was given by Lock (R. & M. 1127[2]) and he was the first to show the equivalence of the flapping and feathering systems. However, the formulae for the coefficients of thrust, flapping amplitudes, etc., in the pure feathering system appear in a different form from the corresponding formulae of the pure flapping system. This is entirely due to the definition of reference axes but it can lead to considerable confusion in the interpretation of the two systems of control application. It is therefore worth while at this stage to clarify the mathematical equivalence of the two systems.

A diagrammatic representation of the pure flapping and pure feathering systems is given in Fig. 2. In the flapping system the axes of reference are the rotor shaft and the plane through the flapping hinges perpendicular to the shaft. In the feathering system, the fundamental axis is that of the rotor disc. It follows that the axes of the pure flapping system are inclined by an angle a_1 with respect to the axes of the pure feathering system.

Denoting the pure flapping system by suffix A and the pure feathering system by suffix B, the comparison of the two systems is as follows.

The resultant air flow at the rotor disc is the same in both cases but by definition of the axes the components of the flow parallel to the axes (and perpendicular to the axes) of the two systems will differ.

To a first approximation

$$\mu_A = \mu_B = \mu \quad .. \quad .. \quad .. \quad .. \quad .. \quad .. \quad .. \quad (25)$$

and

$$\lambda_A = \lambda_B + \mu a_1 . \quad .. \quad .. \quad .. \quad .. \quad .. \quad .. \quad .. \quad (26)$$

Similarly,

$$T_A = T_B = T \quad .. \quad .. \quad .. \quad .. \quad .. \quad .. \quad .. \quad (27)$$

$$Q_A = Q_B = Q \quad .. \quad .. \quad .. \quad .. \quad .. \quad .. \quad .. \quad (28)$$

$$H_A = H_B + Ta_1 . \quad .. \quad .. \quad .. \quad .. \quad .. \quad .. \quad .. \quad (29)$$

For pure flapping (R. & M. 1127[2]), it has been shown

$$a_1 = 2\mu \frac{\frac{4}{3}\vartheta_0 - \lambda_A}{1 - \frac{1}{2}\mu^2} \quad .. \quad .. \quad .. \quad .. \quad .. \quad .. \quad .. \quad (30)$$

while it has been shown in equations (15) and (18) of this report that for pure feathering

$$B_1 = 2\mu \frac{\frac{4}{3}\vartheta_0 - \lambda_B}{1 + \frac{3}{2}\mu^2} . \quad .. \quad .. \quad .. \quad .. \quad .. \quad .. \quad .. \quad (31)$$

By substitution for λ_A or λ_B from equation (26) it can easily be checked that equations (30) and (31) are identical and as shown in equation (21)

$$a_1 = B_1 . \quad .. \quad .. \quad .. \quad .. \quad .. \quad .. \quad .. \quad .. \quad (19)$$

4. *Longitudinal Trim of Helicopter.*—4.1. The previous section dealt with the feathering required to trim the rotor alone in steady rectilinear flight. The feathering required to trim the complete helicopter will now be analysed.

The reference axes are taken as the rotor shaft and the line perpendicular to the rotor shaft passing through the centre of gravity. The aerodynamic drag and pitching moment of the helicopter (less rotor) are referred to the point of intersection O. Such a definition has the advantage of being independent of the centre of gravity position, although for most helicopters the mean centre of gravity position corresponds to the point O and in any case the difference in centre of gravity position from O would be small. The aerodynamic drag and pitching moment include the reactions of any tail surfaces that may be fitted. To generalise the analysis further, the flapping hinges are given an offset from the rotor axis.

For steady rectilinear flight along a path inclined at an angle τ to the horizon, the diagram of forces and moments is as given in Fig. 3. The angles a_1, B_1 and θ are small and the following equations are obtained.

For forces in the vertical direction

$$W + D \sin \tau = T . \qquad .. \quad .. \quad .. \quad .. \quad .. \quad (32)$$

For forces in the horizontal direction

$$D \cos \tau + H = T(B_1 - a_1 - \theta) . \qquad .. \quad .. \quad .. \quad .. \quad (33)$$

For moments about the point O

$$Wf - M_f + M_s(B_1 - a_1) + Th(B_1 - a_1) - Hh = 0 . \qquad .. \quad .. \quad .. \quad .. \quad (34)$$

θ is the angle between the longitudinal axis of the helicopter and the horizon, *i.e.*, the tilt of the helicopter.

a_1 is the flapping amplitude due to forward speed and is equal to the backward tilt of the rotor disc from the no-feathering axis.

B_1 is the feathering amplitude equal to the longitudinal tilt of the no-feathering axis from the shaft axis. This forward tilt of the no-feathering axis is normally proportional to the longitudinal stick displacement. It is a measure of the longitudinal trim of the helicopter analogous to the elevator angle to trim for the fixed-wing aeroplane. The value of B_1 can be obtained from equation (34) in the form

$$B_1 = a_1 + \frac{Hh}{M_s + Th} - \frac{Wf}{M_s + Th} + \frac{M_f}{M_s + Th} . \qquad .. \quad .. \quad .. \quad (35)$$

The majority of present-day helicopters have zero offset hinges so that $M_s = 0$ and equation (35) simplifies in such cases to

$$B_1 = a_1 + \frac{H}{T} - \frac{W}{T}\frac{f}{h} + \frac{M_f}{Th} . \qquad .. \quad .. \quad .. \quad .. \quad .. \quad (36)$$

For all practical cases of steady flight on the helicopter, the thrust is equal to the weight to a very close approximation and equation (36) may therefore be further simplified to the form

$$B_1 = a_1 + \frac{H}{W} - \frac{f}{h} + \frac{M_f}{Wh} . \qquad .. \quad .. \quad .. \quad .. \quad .. \quad .. \quad (37)$$

4.2. For the type of helicopter controlled by application of blade feathering, *i.e.*, for most of the existing helicopters, the longitudinal stick displacement to trim, being a measure of the longitudinal tilt of the no-feathering axis, is (from equation 37) mainly a function of the rotor characteristics $a_1 + H/W$. The position of the centre of gravity influences only the initial position of the stick or, to consider it from another aspect, the trim curves for the helicopter at various centre of gravity positions are parallel. This assumes no change in fuselage pitching moment for the small changes in attitude involved.

The effect of the aerodynamic pitching moment of the fuselage M_f is very difficult to estimate, especially in the presence of the rotor downwash. It is thought that, for a streamlined fuselage without a horizontal tail surface and in autorotation conditions, the effect of M_f is very small. However, in power-on conditions the changes of pitching moment with forward speed could be quite large, taking into account the changes in direction of the slipstream. With increase in forward speed, the direction of the slipstream changes from vertical in hovering flight to almost horizontal at high forward speed. For a helicopter of normal configuration, *e.g.*, the Sikorsky S–51, the pitching moment on the fuselage is nose-up in hovering and low speed changing to nose-down at higher forward speed. Generally it might be said that in power-on conditions the effect of M_f is to decrease the required longitudinal movement of the stick to trim for a given change in speed. The experimental results discussed later would appear to confirm the above arguments.

The effect of a fixed horizontal tail surface could be quite large but the magnitude and direction by which it would alter the stick position to trim will depend largely on the position of the tailplane, particularly in relation to the changes in rotor downwash direction with forward speed.

A further influence which can bring about changes in the tilt of the no-feathering axis (or stick position) is the torsional flexibility of the blade in conjunction with the aerodynamic pitching moment of the blade aerofoil section. For symmetrical section blades the effect should be small but for blades with $C_{m_0} < 0$ as in the case of cambered sections the required stick movements to trim are reduced. This effect increases with forward speed and may even lead to reverse stick movements to trim. An analysis of this particular aspect of the subject will be given in a later report.

4.3. Considering equation (37) in a much wider sense, it will be seen that the helicopter can be trimmed for any given speed by means other than changes of the feathering amplitude or equivalent tilting of the rotor hub. For a constant value of B_1 the helicopter could be trimmed by changes in the centre of gravity position, represented in equation (37) by changes in the value of f/h. This method is actually employed on the small American Seibel helicopter, where control and trim are achieved by fore-and-aft movement of the centre of gravity relative to the rotor shaft, *i.e.*, by variation in the value of f.

Another method of trimming the helicopter is by changing the value of the pitching moment M_f. This could be done by means of an adjustable tail surface, although it is likely to be extremely poor at low forward speed. The use of a horizontal tail rotor with adjustable pitch is a much more practical proposition. The experimental French helicopter SE.3101[16] uses tail rotors to trim the helicopter longitudinally.

4.4. Fig. 4 gives a diagrammatic representation of the theoretical values of B_1 as a function of forward speed, neglecting the aerodynamic moment of the fuselage and assuming no blade twist. Since the longitudinal tilt of the no-feathering axis is proportional to stick displacement, the slope of the B_1 curve might be regarded as the measure of the helicopter stick-fixed static stability. This is analogous to fixed-wing aeroplane practice where the slope of the curve of elevator angle to trim is proportional to the stick-fixed static stability. It is not within the scope of this report to discuss static stability considerations in detail but some explanation is useful in relation to the stick position to trim.

From equation (37) differentiating with respect to forward speed and remembering that thrust is constant along a trim curve, *i.e.*, taking the slope of the B_1 curve of Fig. 4.

$$\frac{\partial B_1}{\partial V} = \frac{\partial a_1}{\partial V} + \frac{1}{W}\frac{\partial H}{\partial V} + \frac{1}{Wh}\frac{\partial M_f}{\partial V}. \qquad \ldots \quad (38)$$

Now, an investigation of the dynamic stability characteristics of the helicopter[4], shows that the constant term of the frequency equation defining the stick-fixed longitudinal stability is of the form

$$D = \frac{gWh}{I}\left[\frac{\partial a_1}{\partial V} + \frac{1}{W}\frac{\partial H}{\partial V} + \frac{1}{Wh}\frac{\partial M_f}{\partial V}\right]. \quad .. \quad .. \quad .. \quad .. \quad (39)$$

This equation has been rewritten from equation (25) of Ref. 4, omitting the part referring to the offset hinge effect but including the fuselage pitching moments.

Thus, comparing (38) and (39) we find that the slope of the control angle curve is proportional to the constant term in the solution of the equations of motion under stick-fixed conditions and is therefore the measure of the static stability of the helicopter.

It is known that large moments are introduced by rapid angular displacement of the rotor and it is advisable to give a more detailed explanation of the relationship of this to the static stability dealt with above. Considering the moments produced by sudden angular displacement of the rotor, we find that these moments are destabilising. For example, decrease in the angle of attack of the rotor, *i.e.*, tilting the rotor backwards decreases the flow through the disc (λ) and by equation (23) this will cause an increase in the flapping amplitude a_1 thus tilting the disc further back and producing a destabilising moment on the helicopter. This form of static instability due to angular displacements is zero in hovering flight and generally increases with increase in forward speed, becoming very important at high speed.

This is only true if the collective pitch is kept constant. If the change in rotor angle of attack is made with the appropriate change in collective pitch to maintain a constant thrust, the conditions are determined by equations (12) and (23) and the pitching moments virtually disappear. Thus, for static stability defined in terms of conditions along a trim curve (thrust constant) the effect of the pitching-moment variation with attitude does not arise and the static stability is as evaluated from equations (38) or (39).

5. *Lateral Trim of Helicopter.*—5.1. A lateral tilt of the no-feathering axis of the helicopter rotor is required to counteract the lateral tilt of the tip-path plane due to flapping motion at forward speed. In addition, for single-rotor helicopters of the Sikorsky configuration, where the tail rotor provides torque reaction compensation, a side force from the main rotor is necessary to compensate for the tail rotor thrust.

By a similar method to that used in section 4 for deriving the control angle for longitudinal trim, the lateral forces and moments about the longitudinal axis give the lateral tilt of the no-feathering axis to trim the helicopter. Due to the more symmetrical conditions in the lateral trim the equations are simpler. The lateral component of the main rotor thrust equals the tail rotor thrust T_t.

$$T(A_1 + b_1 - \phi) = -T_t \quad .. \quad .. \quad .. \quad .. \quad .. \quad (40)$$

and the moments give

$$Wf_1 + T_t h_t + Th(A_1 + b_1) = 0 \quad .. \quad .. \quad .. \quad .. \quad .. \quad (41)$$

where ϕ is the angle of bank of the helicopter

f_1 is the lateral offset of the centre of gravity

h_t is the height of the tail rotor axis above the origin of the helicopter axes.

Hence the lateral tilt of the no-feathering axis A_1, proportional to the lateral stick displacement, can be evaluated from equation (41)

$$A_1 = -b_1 - \frac{Wf_1}{Th} - \frac{T_t h_t}{Th}. \quad .. \quad .. \quad .. \quad .. \quad .. \quad .. \quad (42)$$

Again, this may be simplified in some cases by putting the thrust equal to the weight and for most layouts of normal configuration the tail rotor height is approximately equal to the main rotor height (i.e., $h_t = h$).

Therefore $$A_1 = -b_1 - \frac{f_1}{h} - \frac{T_t}{W}. \qquad (43)$$

Thus for the helicopter with feathering control, the lateral stick displacement to trim is a function of the rotor characteristic b_1 which has been evaluated in equation (24). The effect of the centre of gravity position only affects the initial trim of the helicopter. The effect of the tail rotor thrust is constant under constant torque conditions (or constant power conditions if the engine speed is constant). In autorotation this term disappears.

5.2. The flapping motion of rotor blades was checked experimentally in this country on the autogyro (R. & M. 2505[10]) and more recently in America on helicopters[3,11]. There is excellent agreement in the experimental and theoretical values of a_0 (coning angle) and a_1 (longitudinal tilt). However, the measured values of b_1 (lateral tilt) are much larger than estimated by the above theory.

The angle of side tilt of the rotor disc b_1 is produced by the difference in flow conditions at the various azimuth positions of the blade. This will be evident from equation (8) where the blade angle of attack is expressed in terms of flow through the disc λ, the coning angle a_0 and the blade azimuth position ψ. Most of the existing theories are based on the assumption of constant induced velocity and constant flow through the disc.

Evaluating the expression for b_1 as in equation (24) it may be said in general terms that the side tilt of the rotor disc is due to the flapping motion produced by the difference of blade incidence (maximum in the fore and aft positions introduced by the coning angle).

The effect of slipstream curvature is to increase the difference in blade incidence with azimuth position. Recent work on the visualisation of the flow through the rotor disc in forward flight using a smoke filament technique[17] has shown that the magnitude of the slipstream curvature effect is appreciable, especially when considered in relation to the coning angle used to evaluate b_1 in equation (24).

A very simple method of estimating the order of the slipstream curvature effect can be obtained by considering the ' effective ' increase in coning due to the flow curvature. Referring to the photographs of the flow patterns in Ref. 17 and denoting the angle between the streamline directions at the 0·75-radius sections in the fore and aft positions of the blade by 2δ, the effective coning angle can then be taken as $a_0 + \delta$. Using a case from Ref. 17 as an example, for a coning angle of 7 deg at a tip speed ratio of 0·2, the curvature effect gives a δ of the order of 5 deg. Thus, the slipstream curvature may almost double the value of b_1 based on the simple theory.

The slipstream curvature effect can be treated theoretically on the assumption of a linear increase in induced velocity from front to rear of the disc. Denoting the induced velocity at the rear of the disc to the mean induced velocity by $K + 1$ (as in Refs. 3 and 17) the induced velocity at any point in the disc is given by

$$v_i = v_{i0}(1 + xK \cos \psi) \qquad (44)$$

where v_{i0} is the mean induced velocity.

Inserting the value for induced velocity in the values of flow through the disc λ occurring in equations (6) (7) (8) (9) and (10) it can be shown that the values of a_0 and a_1 as given by equations (13) and (23) respectively remain unchanged but that the value of b_1 [*cf.* equation (24)] now takes the form

$$b_1 = \frac{1}{1 + \frac{1}{2}\mu^2}\left[\tfrac{4}{3}\mu a_0 + \frac{v_{i0}}{\Omega R} K\right]. \qquad (45)$$

Relating v_{i0} to resultant velocity V' in the momentum equation

$$T = 2\pi R^2 \rho V' v_{i0} \quad .. \quad .. \quad .. \quad .. \quad .. \quad .. \quad .. \quad (46)$$

and evaluating V' in the form

$$V' = \Omega R\sqrt{(\mu^2 + \lambda^2)} \quad .. \quad .. \quad .. \quad .. \quad .. \quad .. \quad .. \quad (47)$$

equation (45) may be written in the form

$$b_1 = \frac{1}{1 + \frac{1}{2}\mu^2}\left[\tfrac{4}{3}\mu a_0 + \frac{K\sigma t_c}{2\sqrt{(\mu^2 + \lambda^2)}}\right]. \quad .. \quad .. \quad .. \quad .. \quad (48)$$

5.3. The flapping motion of rotor blades, as obtained on the R–4B helicopter[3] and on the C–30 autogyro (R. & M. 1859[8]), was measured by means of a camera located on the rotor head. This is undoubtedly one of the most reliable methods of test and the accuracy of results by such a method is assured.

In Fig. 5, the measured values of b_1 for the R–4B helicopter are plotted, together with the theoretical estimates made by simple theory and also by taking into account the slipstream curvature effect as obtained in the flight tests of Ref. 17. The graph shows the magnitude of the slipstream curvature effect and the excellent agreement with the flight results when this effect is taken into consideration.

In Fig. 6, similar results are plotted for the C–30 autogyro. Unfortunately there are no flight results of the flow patterns under autorotation conditions at forward speed but the helicopter flow effect as mentioned above is used for comparison. As the accuracy of the flapping measurements is considered to be very good, the results for b_1 can be interpreted as giving some indication of the autorotational flow conditions in existence. This shows that the slope of the induced velocity distribution is considerably less than in helicopter flight. This would be expected from consideration of the small flow through the disc in autorotation. These results give the order of the flow effect to be taken into account for the helicopter under autorotation conditions.

6. *Helicopter Attitude in Forward Flight.*—The attitude of the helicopter, measured as the angle of the rotor shaft to the vertical, can be found from equations (32) (33) (34) and is given in the general case by

$$\theta = -\frac{D}{T}\cos\tau - \frac{H}{T} + (B_1 - a_1) \quad .. \quad .. \quad .. \quad .. \quad .. \quad (49)$$

which can be evaluated

$$\theta = -\frac{D}{T}\cos\tau - \frac{M_s}{M_s + Th}\frac{H}{T} - \frac{Wf}{M_s + Th} + \frac{M_f}{M_s + Th}. \quad .. \quad (50)$$

Simplifying for the helicopter with zero offset hinges and putting the thrust equal to the weight, equation (50) becomes

$$\theta = -\frac{D}{W}\cos\tau - \frac{f}{h} + \frac{Mf}{Wh}. \quad .. \quad .. \quad .. \quad .. \quad .. \quad .. \quad (51)$$

It will be seen that the helicopter takes a nose-down attitude in forward flight unless large pitching moments are applied from the fuselage. The angle is mainly defined by the helicopter drag and increases roughly as the square of the forward speed. The centre of gravity position has only an initial effect on attitude which does not vary with forward speed.

It is interesting to note that the helicopter attitude in space is mainly a function of forward speed and is very little affected by the flight path direction. Thus, for a given forward speed, the attitude is independent of whether the helicopter is climbing, flying level or descending.

This point is of importance in considering the general handling characteristics of the helicopter and in certain particular features of the work, such as the use of the artificial horizon in blind flying.

Similar to the above method, the lateral tilt of the helicopter fuselage can be found from equations (40) and (41) from the form

$$\phi = A_1 + b_1 + \frac{T_t}{T} \quad .. \quad .. \quad .. \quad .. \quad .. \quad .. \quad .. \quad (52)$$

and evaluating

$$\phi = -\frac{W}{T}\frac{f_1}{h} - \frac{T_t}{T}\frac{h_t}{h} + \frac{T_t}{T} . \quad .. \quad .. \quad .. \quad .. \quad .. \quad (53)$$

Making the usual approximation that the thrust equals the weight and taking the general configuration where the tail-rotor height is approximately the main-rotor height, the lateral tilt of the helicopter fuselage can be simplified to

$$\phi = -f_1/h . \quad .. \quad .. \quad .. \quad .. \quad .. \quad .. \quad .. \quad .. \quad (54)$$

Thus, the lateral tilt of the helicopter fuselage for the orthodox configuration is simply that due to the centre-of-gravity offset.

7. *Comparison of Theory and Flight Tests.*—7.1. *General.*—A comparison is made of the theory with available flight information on two types of helicopter. For the R–4B helicopter, the flight results are taken from R. & M. 2431[5] and from further unpublished work. Some American results are also included. For the S–51 helicopter the results are taken mainly from Ref. 18.

The blade-pitch distribution as measured in the flight tests has been analysed using the expression for blade angle as given in equation (3)

$$\vartheta = \vartheta_0 - A_1 \cos \psi - B_1 \sin \psi . \quad .. \quad .. \quad .. \quad .. \quad .. \quad (3)$$

The comparison is then made for the three coefficients, ϑ_0 the collective blade pitch, A_1 representing the lateral control and B_1 representing the longitudinal control. The analysis is strictly in relation to the helicopter axes and hence the longitudinal control B_1 may not correspond identically with fore-and-aft movement of the stick.

However, there is a further effect which must be taken into account in making this analysis. The blades are connected to the rotor hub by two pin-joints, *viz.*, the horizontal flapping hinge and the vertical drag hinge. In section 2 of this report it was shown that the blade flapping position with respect to the flapping hinge was obtained in the form of a coning angle derived as the equilibrium position for the moments of the aerodynamic lift forces and of the centrifugal forces about the flapping hinge. In the same way, the position of the blade in relation to the drag hinge is obtained from the moments of the lift and drag components and of the centrifugal force. The drag angle, *i.e.*, the angle between the longitudinal axis of the blade and the plane through the axis of rotation and the drag hinge, depends therefore on the pitch and power applied to the blades. In autorotation the angle is practically zero and as pitch and power are applied the blade drags back depending on the moment from the components of the lift and drag forces. As the blade moves round the drag hinge, it changes its angle with respect to the flapping hinge. The arrangement of the drag hinge in relation to the rotor head layout determines the drag angle at which the blade axis is perpendicular to the flapping hinge.

If the blade is not at right-angles to the flapping hinge, flapping motion of the blade produces a change in blade pitch or what is known as a delta-3 hinge effect, the delta-3 angle in this case being due to the difference in the angle of the blade axis to the flapping hinge from the 90 deg position. If the blade is ahead of the right-angle position, upward flapping causes a decrease in blade pitch while if the blade is back from the right-angle position, upward flapping causes an increase in blade angle. Now, this latter condition can lead to serious blade instability and the

range of blade travel about the drag hinge must be arranged to avoid such a case by appropriate positioning of the drag hinge. Thus, it is usually found that the blade is approximately at right-angles to the flapping hinge at the highest permissible power condition and as autorotation is approached the blade moves forward about the drag hinge and introduces a delta-3 effect. This effect of pitch change produced by flapping motion is dealt with in Ref. 18 for the S–51 helicopter.

The effect of the delta-3 hinge configuration is to introduce a phase angle between the feathering applied to the blades and the associated flapping motion. Alternatively, it may be considered as coupling effects between the longitudinal and lateral control. It will be realised that these effects arise from the flapping of the blades relative to the shaft. In practice, the fore-and-aft tilt of the disc relative to the shaft may be comparatively large (due to fuselage pitching moments, etc.) while the lateral inclination will be relatively small. The introduction of these coupling terms will therefore have very little effect on B_1 but may alter A_1 considerably. The mathematical analysis of the delta-3 hinge configuration and the associated feathering coefficients is treated separately in an appendix.

Another possible influence in the comparison of theoretical and experimental control angles is that twisting of the rotor blades may occur. To investigate this possibility some theoretical work on blade twist was done. It was found that with blade twist the collective pitch, as measured at the root, has to be increased and to a first approximation this increment is independent of forward speed. Also the feathering amplitude to trim (B_1) is reduced by an amount increasing with forward speed. These symptoms were much in evidence in the autogyro work of R. & M. 1859[8] where considerable twisting did take place.

The comparison of the theoretical and experimental values of collective blade pitch and comparison of the values of B_1 for both the R–4B and S–51 helicopters does not indicate the existence of any blade twisting. It should be noted that symmetrical blade sections are used on both of these helicopters and, neglecting blade distortion, the section pitching moments should be negligible.

The evaluation of the lateral tilt of the rotor includes, in the power-on case, a term involving the thrust of the tail rotor. This term is comparatively large and it was therefore advisable to analyse the tail-rotor characteristics. In the simple case, the thrust of the tail rotor can be obtained from the moment about the main rotor axis to compensate the torque reaction of the main rotor, knowing the power input to the latter. However, on analysis it was found that the measured tail-rotor blade angles were not always in agreement with the thrust required for complete torque compensation. The helicopter fuselage is in a spiral slipstream from the main rotor and this produces a yawing moment on the fuselage. The direction of this moment is such as to reduce the moment required from the tail rotor.

If the effect of the spiral slipstream takes the form of a pure couple, the tail-rotor thrust is reduced and so also is the corresponding lateral tilt required from the main rotor. If, on the other hand side forces on the fuselage are introduced the lateral tilt of the main rotor must take these into account.

In practice, there is little effect on the tail-rotor angles in hovering or at high forward speeds but there is a considerable effect at intermediary speeds. The comparison of the tail-rotor pitch settings theoretical and experimental is therefore made and the effect is allowed for in the estimation of the lateral feathering coefficient.

7.2. *Collective Pitch Angles.*—The measured and estimated collective pitch angles for the R–4B and for the S–51 helicopters are given in Figs. 7 and 8 respectively. Both level flight and autorotation conditions are considered and in the case of the S–51 helicopter results are given for two different rotational speeds in the level flight conditions.

The flow through the disc, etc., and the evaluations used in the estimations are identical with the work of R. & M. 1730[1]. No allowance for tip loss nor for induced velocity distribution is made. The value of the lift slope was taken as $5 \cdot 6$. It must be remembered that in autorotation the main rotor has to drive the tail rotor and a certain amount of gearing. This effect is introduced into the power equation in the form of a negative torque coefficient applied to the main rotor.

Comparing the theoretical and experimental collective pitch values, the agreement is very good. Due to neglecting the induced velocity distribution in the power-on case, it is to be expected that experimental values will lie above the theoretical curve near hovering. This effect will disappear with increase in forward speed. The tip loss will increase the experimental values slightly throughout the speed range. Comparison of the results does in fact show these features. In autorotation the agreement is excellent throughout the forward speed range.

7.3. *Longitudinal Control to Trim.*—In the estimation of the longitudinal tilt of the no-feathering axis B_1, the flapping term a_1 can be obtained accurately and has been checked experimentally in flight giving good agreement with the estimated values. The H-force term can be estimated with reasonable accuracy and as it is of small magnitude, any error in H-force has little effect on B_1. The centre of gravity effect is simply geometrical. Each of the terms in the expression for B_1 can therefore be estimated accurately except for the fuselage pitching moment. It is therefore more suitable to compare the experimental results with the estimations, excluding fuselage pitching moment and the difference in values then represents the fuselage pitching moment. The latter can then be compared with expected fuselage pitching moments in the various conditions and for the particular case of hovering where estimation is possible.

The longitudinal control to trim for the R–4B helicopter is given in Figs. 9 and 10 for level flight and autorotation conditions respectively. The results of the N.A.C.A. tests with the camera located on the rotor head giving direct measurement[3] are also included. The theoretical curves used for comparison are estimated without fuselage pitching moment, as mentioned above.

Similar curves for the S–51 helicopter are given in Figs. 11 and 12 for level flight at two different rotor speeds and in Fig. 13 for autorotation conditions. The corresponding theoretical curves are also included.

Comparing the theoretical and experimental values, it will be seen that the fuselage pitching moment has a very important effect on the longitudinal control angles required to trim the helicopter in steady conditions. The general influence is more important at low speed in the power-on conditions where the vertical induced velocity causes a large nose-up pitching-moment effect. As the forward speed increases, the fuselage pitching moment decreases until at high speed, where the slipstream effects become negligible, the pitching moment is becoming negative as would be expected. In autorotation, the fuselage influence is much smaller.

To study these effects more fully the fuselage pitching moments as determined from the difference in the theoretical and experimental curves have been plotted in Figs. 14 to 18 for the various conditions considered in Figs. 9 to 13 respectively. The same scales have been used, so that the pitching moments are in non-dimensional form.

The R–4B results (Fig. 14) show quite a large change in fuselage pitching moment with attitude. The general shape of the curves is as would be expected, but the measurements were made during general handling work and may not be sufficiently accurate to define the magnitude of such an influence as change of pitching moment due to attitude. The pitching moments show much less variation with forward speed in autorotation conditions (Fig. 15) but the effect of attitude change is still present. It should be remembered that the upper, lower and side panels of the R–4B fuselage are flat, forming a simple rectangular fuselage section. Such a shape could lead to large fuselage effects as was evident for example in the dynamic stability work of R. & M. 2505[10]. Too much emphasis should not be placed on the R–4B results as it is not typical for fuselage shapes to be expected in the future.

The deduced fuselage pitching moments for the S–51 helicopter are given in Figs. 16, 17 and 18. Change of attitude over a small range has no significant effect as shown by the fact that the points for the different centre-of-gravity positions lie on one curve. The tests at the two different rotor speeds have been plotted separately, but comparison of Figs. 16 and 17 shows that there is no effect on pitching moment. It would not be expected that the difference in flow conditions would be sufficient to influence the pitching moments for the range of rotor speeds considered.

The fuselage pitching moment is nose-up in hovering flight due to the vertical induced velocity. This particular case can be estimated fairly accurately and the magnitude of the estimation is in excellent agreement with the measurements. As forward speed increases, the nose-up pitching moment decreases and becomes negative at high forward speed. The slipstream now has little effect and the negative pitching moment is as would be expected from measurements on aircraft fuselages.

In autorotation, the fuselage pitching moment remains constant with forward speed. The undercarriage stub arrangement contributes to the nose-up pitching moment in autorotation. The difference in fuselage pitching moments at high speed for level flight and autorotation are due to the large changes in flow relative to the fuselage.

7.4. *Lateral Control to Trim.*—The lateral control to trim the helicopter is given in Figs. 19 and 20 for the R–4B in level flight and autorotation conditions respectively. The theoretical estimations are based on the work of section 5, including slipstream curvature and tail-rotor thrust based on experimental tail-rotor pitch measurements.

In Fig. 21, flight tests on the measurement of tail-rotor pitch angles from R. & M. 2431[5] are compared with the pitch angles that would be required to give full compensation for the reaction of the torque at the main rotor. The estimation of tail-rotor pitch angles is made similar to the collective pitch evaluation for the main rotor and there is therefore no need to repeat the details of the method. In practice the tail-rotor angles (and therefore the tail-rotor thrust) are much smaller than would be required for full torque reaction compensation. This means that the spiral slipstream must be producing a moment on the fuselage countering the torque reaction. It is easy to check that the direction of the moment from the slipstream is in the correct sense but evaluation of the magnitude is virtually impossible.

Comparison of experimental and theoretical values of A_1 in both the level flight and autorotation conditions gives very good agreement. In autorotation the estimation corresponds exactly with the measurements while in the power-on case the small discrepancy could easily be accounted for by small side forces on the fuselage from a small angle of sideslip or from the spiral slipstream effect.

Similar curves for the lateral control to trim on the S–51 helicopter are given in Figs. 22 and 23 for level flight at two rotor speeds and in Fig. 24 for autorotation conditions. A comparison of measured tail-rotor pitch angles with the angles estimated to give full torque reaction compensation is made in Fig. 25. In this case, the experimental and estimated tail-rotor pitch angles are in good agreement. Thus, we again find that the streamlined shape of the S–51 compared with the R–4B gives a much smaller fuselage moment effect.

Comparing the experimental and theoretical values of A_1 we find excellent agreement in the autorotation case. In the level flight conditions, the lateral trim is overestimated by about 0·75 deg at the higher rotor speed and about 1 deg at the lower rotor speed. The most likely reason for this discrepancy is the inability to estimate side forces on the fuselage due to the spiral nature of the slipstream. It has been shown that yawing moments due to the slipstream can be checked by consideration of the tail-rotor thrust to maintain equilibrium. However, side forces on the fuselage have a direct effect on the tilt required from the main rotor and there is no simple way of determining the existence of such forces or of evaluating their magnitude. The greatest discrepancy in the results, *viz.*, 1 deg, is equivalent to a side force of 80 lb which is within the possible value that could be expected from the slipstream spiral flow or from a small angle of sideslip. Although precautions were taken to eliminate possible error due to the latter, absolute measurement on the helicopter is difficult and a small angle of sideslip could occur. It is interesting to note that while zero sideslip on the fixed-wing aeroplane is necessarily associated with zero bank for straight flight, the helicopter does not necessarily conform to this due to the additional freedom between the rotor and the fuselage.

7.5. *Helicopter Attitude.*—Fig. 26 gives the experimental results for the shaft attitude in forward flight on the R–4B helicopter[6] and these are compared with the theoretical estimation based on a drag of 240 lb at 100 ft/sec. A detailed estimate of this drag value was given in Ref. 6 but it should be remembered that changes of attitude or of slipstream could cause large variations in this drag.

The agreement is good in general in showing the trend of the helicopter attitude with forward speed but the experimental results have too great a scatter to allow a more accurate comparison to be made.

The attitude curves for the S–51 helicopter are given in Figs. 27 and 28 for level flight and autorotation conditions respectively. The experimental results are taken from Ref. 18 and the theoretical curves are based on a drag of 300 lb at 100 ft/sec.

The agreement is good and the discrepancies are associated with the fuselage pitching moments. This latter effect should correspond with that obtained from the feathering amplitude work. However, the numerical values for pitching moment in the two cases are not in good agreement but this is mainly due to the difficulty in estimating drag of the fuselage with the required accuracy. For this fuselage shape and considering the changes in fuselage attitude and slipstream direction with forward speed, the drag will vary in a complex manner. It is therefore an unsuitable method to deduce pitching-moment data from attitude curves.

8. *Conclusions.*—(*a*) The equivalence of the flapping and feathering systems of helicopter rotor control has been shown mathematically and also from the simple physical aspect.

(*b*) The feathering or flapping required to trim a rotor disc for equilibrium in forward flight has been evaluated. The variation of induced velocity over the disc has an important effect on the lateral tilt of the disc.

(*c*) The feathering required to trim the helicopter in forward flight has been evaluated.

(*d*) Comparison of the estimated longitudinal trim (B_1 longitudinal tilt of the no-feathering axis) with experimental results gives good agreement. The main difficulty is in the estimation of fuselage pitching moments in the presence of the rotor slipstream.

(*e*) Comparison of the estimated lateral trim (A_1 lateral tilt of the no-feathering axis) with experimental results gives good agreement. The effects of slipstream curvature and of the tail-rotor behaviour are important.

(*f*) The attitude of the helicopter in forward flight is estimated and is mainly a function of fuselage drag. Agreement with flight measurement is satisfactory.

(*g*) A delta-3 hinge introduces coupling effects on the feathering and flapping amplitudes. This is dealt with in an appendix.

REFERENCES

No.	Author	Title, etc.
1	H. B. Squire	The Flight of a Helicopter. R. & M. 1730. November, 1935.
2	C. N. H. Lock	Further Developments of Autogyro Theory. R. & M. 1127. March, 1927.
3	G. C. Myers	Flight Measurements of Helicopter Blade Motion with a Comparison between Theory and Experimental Results. N.A.C.A. Tech. Note 1266. April, 1947.
4	J. K. Zbrozek	Introduction to Dynamic Longitudinal Stability of Single-rotor Helicopter with Hinged Blades. A.R.C. 11,440. February, 1948.
5	W. Stewart	General Handling Tests on the Sikorsky R–4B Helicopter (*Hoverfly* I). R. & M. 2431. October, 1946.
6	W. Stewart	Brief Performance Tests on the *Hoverfly* I by Aneroid Method and Flight Path Recorder. A.R.C. 10,733. May, 1947.
7	J. A. Beavan and C. N. H. Lock ..	The Effect of Blade Twist on the Characteristics of the C-30 Autogyro. R. & M. 1727. April, 1936.
8	P. A. Hufton, A. E. Woodward Nutt, F. J. Biggs, and J. A. Beavan ..	General Investigation into the Characteristics of the C–30 Autogyro. R. & M. 1859. March, 1939.
9	H. Glauert	A General Theory of the Autogyro. R. & M. 1111. November, 1926.
10	W. Stewart	Dynamic Longitudinal Stability Measurements on the Sikorsky R–4B Helicopter (*Hoverfly* Mk. I). R. & M. 2505. February, 1948.
11	E. Migotsky	Full Scale Investigation of the Blade Motion of the PV–2 Helicopter Rotor. N.A.C.A. Tech. Note 1521. March, 1948.
12	E. Migotsky	Full Scale Tunnel Performance Tests of the PV–2 Helicopter Rotor. N.A.C.A. Report Memorandum L5C29a.
13	P. Brotherhood	An Investigation in Flight of the Induced Velocity Distribution under a Helicopter Rotor when Hovering. R. & M. 2521. June, 1947.
14	J. S. Glass and H. A. Mather	Sikorsky S–51 Performance and Handling Tests. A.R.C. 11,238.
15	F. J. Bailey	A Simplified Theoretical Method of Determining the Characteristics of a Lifting Rotor in Forward Flight. N.A.C.A. Report 716. 1941.
16	—	Helicopter SE–3101. *Aeroplane*. 23rd July, 1948.
17	P. Brotherhood and W. Stewart ..	An Experimental Investigation of the Flow through a Helicopter Rotor in Forward Flight. A.R.C. 12,894. (To be published.)
18	P. Brotherhood and M. F. Burle ..	Flight Measurements of Longitudinal and Lateral Trim of the S–51 Helicopter. A.R.C. 12,879.
19	J. K. Zbrozek	Stability and Control of Single Rotor Helicopter with Hinged Blades. *Aircraft Engineering*. February, 1949.

LIST OF SYMBOLS

$a = dC_L/d\alpha$	Lift slope of blade section
a_0	Coning angle
a_1 and b_1	Coefficients in Fourier series for flapping
A_1 and B_1	Coefficients in Fourier series for feathering measured in plane perpendicular to rotor shaft
A_{1D} and B_{1D}	Coefficients in Fourier series for feathering measured in plane of rotor disc
b	Number of blades
c	Blade chord

c	Mean blade chord $= \left(\int_0^R cr^2\,dr\right)\Big/\left(\int_0^R r^2\,dr\right)$
$C_{m\,0}$	Pitching-moment coefficient of blade section
D	Drag of helicopter
e	Distance of flapping hinges from axis of rotation
f	Fore-and-aft position of centre of gravity relative to shaft
f_1	Lateral position of centre of gravity relative to shaft
h	Distance of rotor centre above centre of gravity
H	Longitudinal rotor force parallel to rotor disc
h_c	Coefficient $H/bcR\rho(\Omega R)^2$
I_1	Blade moment of inertia about flapping hinge
M_f	Aerodynamic pitching moment of fuselage
$M_s = \frac{1}{2}Se$	Unit moment due to centrifugal force of all blades
Q	Rotor torque
$r = xR$	Radius of given blade section
R	Rotor radius
S	Centrifugal force of all blades
T	Rotor thrust
t_c	Thrust coefficient $T/bcR\rho(\Omega R)^2$
U	Velocity of flow through the rotor disc
V	Velocity of steady flight
v_i	Induced velocity at given position on disc
$v_{i\,0}$	Mean induced velocity
W	Weight of helicopter
x	Fraction of rotor radius
α	Incidence of blade section
i	Incidence of rotor disc
β	Flapping angle measured from no-feathering plane
β_s	Flapping angle measured from plane perpendicular to shaft
γ_0	Lock's inertia number $(\rho a\bar{c}R^4)/I_1$
θ	Angle of pitch of helicopter from horizon
ϑ	Instantaneous pitch of blade
ϑ_0	Collective pitch of blade
$\lambda = U/\Omega R$	Coefficient of flow through disc
$\mu = (V\cos i)/\Omega R$	Tip speed ratio
ρ	Air density
τ	Angle of climb
ψ	Blade azimuth position measured from the downwind position in direction of rotation
Ω	Angular velocity of rotor

(59987)

APPENDIX I

Effect of Delta-3 Hinge

The considerations of sections 2 and 3 of this report are based on the assumption that the blade axis is at right-angles to the flapping hinge and that flapping motion has therefore no effect on the pitch setting of the blade. In some designs this is not the case and even for the layout with simple flapping and drag hinges variations from the right-angle position do occur.

It has been shown in section 2 that the coning angle of the blades is the position for equilibrium of the lift and centrifugal force moments of the blade about the flapping hinge. In a similar way, freedom about the drag hinge introduces a drag angle which is the equilibrium position for the torque and centrifugal force moment about the drag hinge. This drag angle, *i.e.*, the angle between the longitudinal axis of the blade and the plane through the axis of rotation and the drag hinge, depends therefore on the power conditions for the rotor. In autorotation the angle is practically zero and as pitch and power are applied to the rotor the blades drag back from this position until the centrifugal force moment produces equilibrium.

When the blade is not at right-angles to the flapping hinge, flapping motion of the blade produces a change in blade pitch. If the blade is ahead of the 90 deg position, upward flapping causes a decrease in blade pitch while if the blade is back from the 90 deg position upward flapping causes an increase in pitch. Now, this latter condition can lead to serious blade instability and the range of blade travel about the drag hinge must be arranged to avoid such a possibility by appropriate positioning of the drag hinge. Thus, it is usually found that the blade is almost at right-angles to the flapping hinge at highest permissible power conditions and as autorotation is approached the blade moves forward on the drag hinge and introduces a delta-3 hinge effect. This is illustrated in Fig. 29 where the rotor head configuration for the S–51 helicopter is shown. This diagram will be used to illustrate the effect of the angle (ψ_0) of the blade axis from the right-angle position to the flapping hinge axis on the estimation of the feathering coefficients.

It can be shown from simple mechanics that if the axis of the blade flaps up by an angle β_s the pitch setting of the blade will change by an angle $-\beta_s \tan \psi_0$.

For the general conditions, consider the case where the tip-path plane is maintained constant and the shaft is tilted longitudinally by an angle a_1 and laterally by an angle b_1 so that cyclic flapping of the blades relative to the shaft takes the form

$$-a_{1s} \cos \psi - b_{1s} \sin \psi \,. \qquad .. \quad .. \quad .. \quad .. \quad (55)$$

This introduces a cyclic variation of the flapping hinge setting relative to the tip-path plane in the form

$$-a_{1s} \sin (\psi - \psi_0) + b_{1s} \cos (\psi - \psi_0) \qquad .. \quad .. \quad .. \quad (56)$$

and the cyclic pitch of the blades becomes

$$-a_{1s} \frac{\sin (\psi - \psi_0)}{\cos \psi_0} + b_{1s} \frac{\cos (\psi - \psi_0)}{\cos \psi_0} \qquad .. \quad .. \quad .. \quad .. \quad (57)$$

which can be expanded in the form

$$-a_{1s} \sin \psi + a_{1s} \cos \psi \tan \psi_0 + b_{1s} \cos \psi + b_{1s} \sin \psi \tan \psi_0 \,. \quad .. \quad .. \quad .. \quad (58)$$

Assuming the pitch of the blades is expressed as in equation (3) in the form

$$\vartheta = \vartheta_0 - A_1 \cos \psi - B_1 \sin \psi \qquad .. \quad .. \quad .. \quad .. \quad .. \quad .. \quad .. \quad .. \quad (3)$$

where ϑ_0 is now the collective pitch at a coning angle a_0.

The angle of attack of blade section at radius r, similar to that of equation (8) but introducing expression (58) is given by

$$\alpha = \vartheta_0 - A_1 \cos\psi - B_1 \sin\psi - a_{1s} \sin\psi + a_{1s} \cos\psi \tan\psi_0$$
$$+ b_{1s} \cos\psi + b_{1s} \sin\psi \tan\psi_0 - \frac{u + V \cos i a_0 \cos\psi}{\Omega r + V \cos i \sin\psi} \quad .. \quad .. \quad .. \quad .. \quad (59)$$

and may be rewritten in the form

$$\alpha = \vartheta_0 - (A_1 - b_{1s} - a_{1s} \tan\psi_0) \cos\psi - (B_1 + a_{1s} - b_{1s} \tan\psi_0) \sin\psi$$
$$- \frac{\lambda + \mu a_0 \cos\psi}{x + \mu \sin\psi} . \quad .. \quad .. \quad .. \quad .. \quad .. \quad .. \quad .. \quad .. \quad .. \quad (60)$$

The increment of the aerodynamic moment about the flapping hinge is then

$$dM = \tfrac{1}{2} a \rho c \, dr \, . \, r[\Omega r + V \cos i \sin\psi]^2 \alpha . \quad .. \quad .. \quad .. \quad .. \quad .. \quad .. \quad .. \quad (61)$$

Substituting from equation (60), expanding and integrating between the limits O and R the evaluation of the aerodynamic moment becomes

$$M = \tfrac{1}{2}\rho c a R^4 \Omega^2 [\tfrac{1}{4}\vartheta_0 (1 + \mu^2) + \tfrac{2}{3}\mu\vartheta_0 \sin\psi$$
$$- (A_1 - b_{1s} - a_{1s} \tan\psi_0)\tfrac{1}{4}(1 + \tfrac{1}{2}\mu^2) \cos\psi$$
$$- (B_1 + a_{1s} - b_{1s} \tan\psi_0)\tfrac{1}{4}(1 + \tfrac{3}{2}\mu^2) \sin\psi$$
$$- \tfrac{1}{3}\mu(B_1 + a_{1s} - b_{1s} \tan\psi_0)$$
$$- \frac{\lambda}{3} - \tfrac{1}{2}\lambda\mu \sin\psi - \tfrac{1}{3}\mu a_0 \cos\psi] . \quad .. \quad .. \quad .. \quad .. \quad .. \quad .. \quad (62)$$

The disc is maintained in equilibrium so that this moment must equal the moment due to the centrifugal forces about the flapping hinge.

$$M = I_1 \Omega^2 a_0 . \quad .. \quad .. \quad .. \quad .. \quad .. \quad .. \quad .. \quad .. \quad .. \quad (63)$$

Equating the coefficients, *i.e.*, constant term equal to the centrifugal force moment and coefficients of sin ψ and cos ψ equal to zero,

$$\tfrac{1}{2}\rho c a R^4 \Omega^2 \left[\tfrac{1}{4}\vartheta_0(1 + \mu^2) - \tfrac{1}{3}\mu(B_1 + a_{1s} - b_{1s} \tan\psi_0) - \frac{\lambda}{3}\right] = I_1 \Omega^2 a_0 \quad .. \quad (64)$$

$$\tfrac{2}{3}\mu\vartheta_0 - \tfrac{1}{2}\mu\lambda - (B_1 + a_{1s} - b_{1s} \tan\psi_0) \tfrac{1}{4}(1 + \tfrac{3}{2}\mu^2) = 0 \quad .. \quad .. \quad (65)$$

$$\tfrac{1}{4}(1 + \tfrac{1}{2}\mu^2)(A_1 - b_{1s} - a_{1s} \tan\psi_0) + \tfrac{1}{3}\mu a_0 = 0 . \quad .. \quad .. \quad (66)$$

Hence,

$$B_1 + a_{1s} - b_{1s} \tan\psi_0 = 2\mu \frac{\frac{4}{3}\vartheta_0 - \lambda}{1 + \frac{3}{2}\mu^2} \quad .. \quad .. \quad .. \quad .. \quad (67)$$

and

$$A_1 - b_{1s} - a_{1s} \tan\psi_0 = -\frac{4}{3} \frac{\mu a_0}{1 + \frac{1}{2}\mu^2} . \quad .. \quad .. \quad .. \quad .. \quad (68)$$

Substituting from (67) in (64) and evaluating

$$a_0 = \frac{\gamma}{2}\left[\tfrac{1}{4}\vartheta_0 \frac{1 - \frac{1}{18}\mu^2 + \frac{3}{2}\mu^4}{1 + \frac{3}{2}\mu^2} - \tfrac{1}{3}\lambda \frac{1 - \frac{1}{2}\mu^2}{1 + \frac{3}{2}\mu^2}\right] . \quad .. \quad .. \quad .. \quad .. \quad .. \quad (69)$$

This value of coning angle is identical with the value derived in equation (13). It must be remembered that in equation (69) the value of ϑ_0 is the collective pitch at the appropriate coning angle whereas in equation (13) the value of ϑ_0 is independent of the flapping conditions.

Considering the right-hand side of equations (67) and (68) it will be seen that these values correspond identically with the flapping coefficients as derived in equations (23) and (24) respectively. Substituting these flapping coefficients, equations (67) and (68) may be transformed into values for B_1 and A_1

$$B_1 = a_1 - a_{1s} + b_{1s} \tan \psi_0 \quad .. \quad .. \quad .. \quad .. \quad .. \quad .. \quad (70)$$

and

$$A_1 = - b_1 + b_{1s} + a_{1s} \tan \psi_0 . \quad .. \quad .. \quad .. \quad .. \quad .. \quad .. \quad (71)$$

a_{1s} and b_{1s} can be evaluated for the helicopter by rewriting the equations of motion, *i.e.*, equations (32), (33) and (34) obtained from Fig. 3, in the form

$$W + D \sin \tau = T \quad .. \quad .. \quad .. \quad .. \quad (72)$$

$$D \cos \tau + H = T(- a_{1s} - \theta) \quad .. \quad .. \quad (73)$$

$$Wf - M_f + M_s(- a_{1s}) + Th(- a_{1s}) - Hh = 0 . \quad .. \quad .. \quad .. \quad .. \quad (74)$$

Hence

$$- a_{1s} = \frac{Hh}{M_s + Th} - \frac{Wf}{M_s + Th} + \frac{M_f}{M_s + Th} . \quad .. \quad .. \quad .. \quad .. \quad (75)$$

Simplying as before

$$- a_{1s} = \frac{H}{W} - \frac{f}{h} + \frac{M_f}{Wh} . \quad .. \quad .. \quad .. \quad .. \quad .. \quad .. \quad .. \quad (76)$$

For the lateral equations of motion

$$T(b_{1s} - \phi) = - T_t \quad .. \quad .. \quad .. \quad .. \quad .. \quad .. \quad .. \quad .. \quad .. \quad (77)$$

$$Wf_1 + T_t h_t + Thb_{1s} = 0 . \quad .. \quad .. \quad .. \quad .. \quad .. \quad .. \quad .. \quad .. \quad .. \quad (78)$$

Hence

$$b_{1s} = - \frac{W}{T} \frac{f_1}{h} - \frac{T_t h_t}{Th} . \quad .. \quad .. \quad .. \quad .. \quad .. \quad .. \quad .. \quad (79)$$

Simplifying

$$b_{1s} = - \frac{f_1}{h} - \frac{T_t h_t}{Wh} . \quad .. \quad .. \quad .. \quad .. \quad .. \quad .. \quad .. \quad (80)$$

Substituting in equations (70) and (71) the feathering coefficients become

$$B_1 = a_1 + \frac{H}{W} - \frac{f}{h} + \frac{M_f}{Wh} + \tan \psi_0 \left(- \frac{f_1}{h} - \frac{T_t h_t}{Wh} \right) \quad .. \quad .. \quad .. \quad (81)$$

and

$$A_1 = - b_1 - \frac{f_1}{h} - \frac{T_t h_t}{Wh} - \tan \psi_0 \left(\frac{H}{W} - \frac{f}{h} + \frac{M_f}{Wh} \right) . \quad .. \quad .. \quad .. \quad (82)$$

Comparing these equations with (37) and (42) the expressions are identical for the first part with the addition of the tan ψ_0 terms, and if the angle ψ_0 becomes zero, equations (81) and (82) take the same form as in the previous work.

In general, the magnitude of the coupling terms are such that there is little effect on B_1 (compared with no delta-3 hinge conditions) but the effect on A_1 can be quite large, particularly if the fuselage pitching moment is of large magnitude. For the normal helicopter layout where the delta-3 hinge effect is small in power-on conditions the influence of the coupling terms is negligible. For the autorotation case, the term involving tail-rotor thrust disappears and since the lateral centre of gravity offset will be very small, there is therefore no alteration to the B_1 amplitude and the effect only appears as an alteration to the A_1 amplitude of feathering.

It must be remembered that throughout this report the feathering amplitudes and the comparison of theoretical and experimental results are associated with the blade position in azimuth as measured from the downwind position, *i.e.*, along the longitudinal axis of the helicopter. The behaviour of the pilot's control in relation to fore-and-aft or lateral displacement is a function of the mechanical linkage to the swash-plate. If pure fore-and-aft stick movement produces pure longitudinal tilt of the swash-plate and also of the no-feathering axis, then the pilot's stick positions fore-and-aft and laterally are directly proportional to the B_1 and A_1 amplitudes respectively. If there is any presetting of the controls the appropriate phase angle must be taken into account when the behaviour of the pilot's controls is considered.

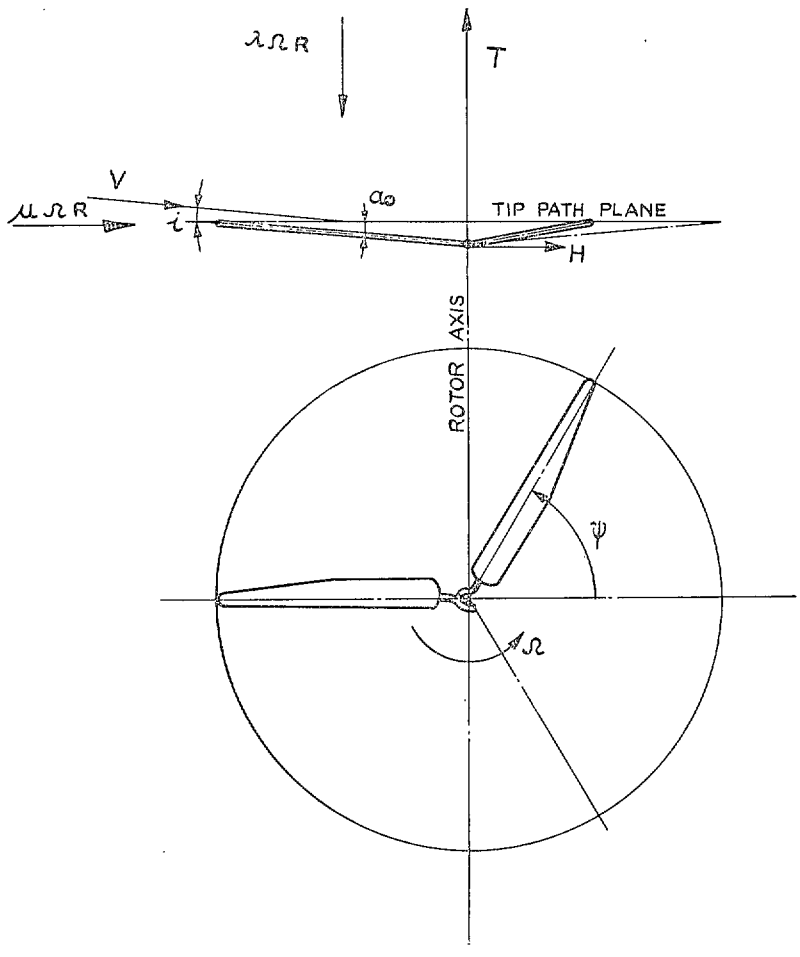

FIG. 1. Rotor disc axis.

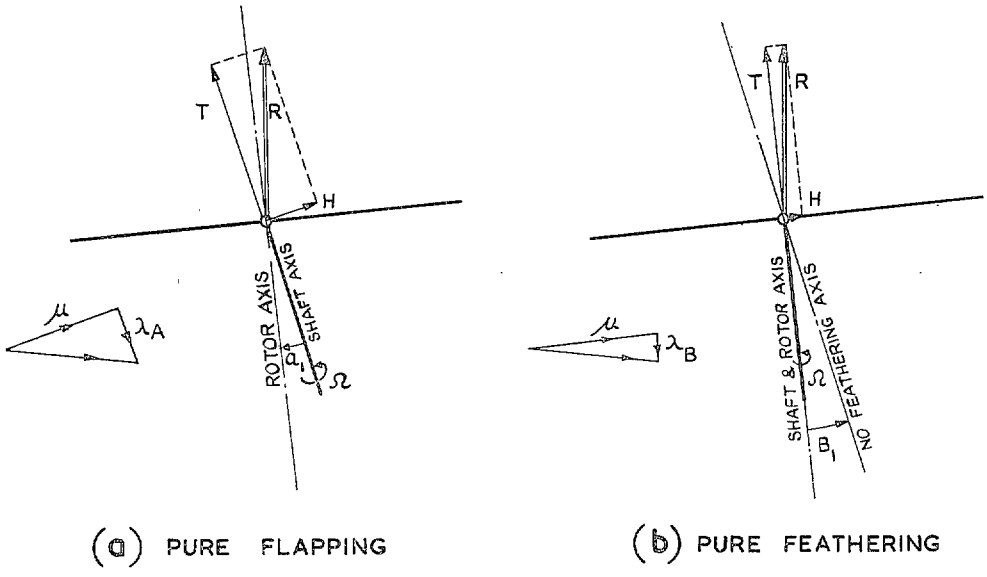

(a) PURE FLAPPING (b) PURE FEATHERING

FIGS. 2a and 2b. Comparison of pure flapping and feathering systems.

(59987)

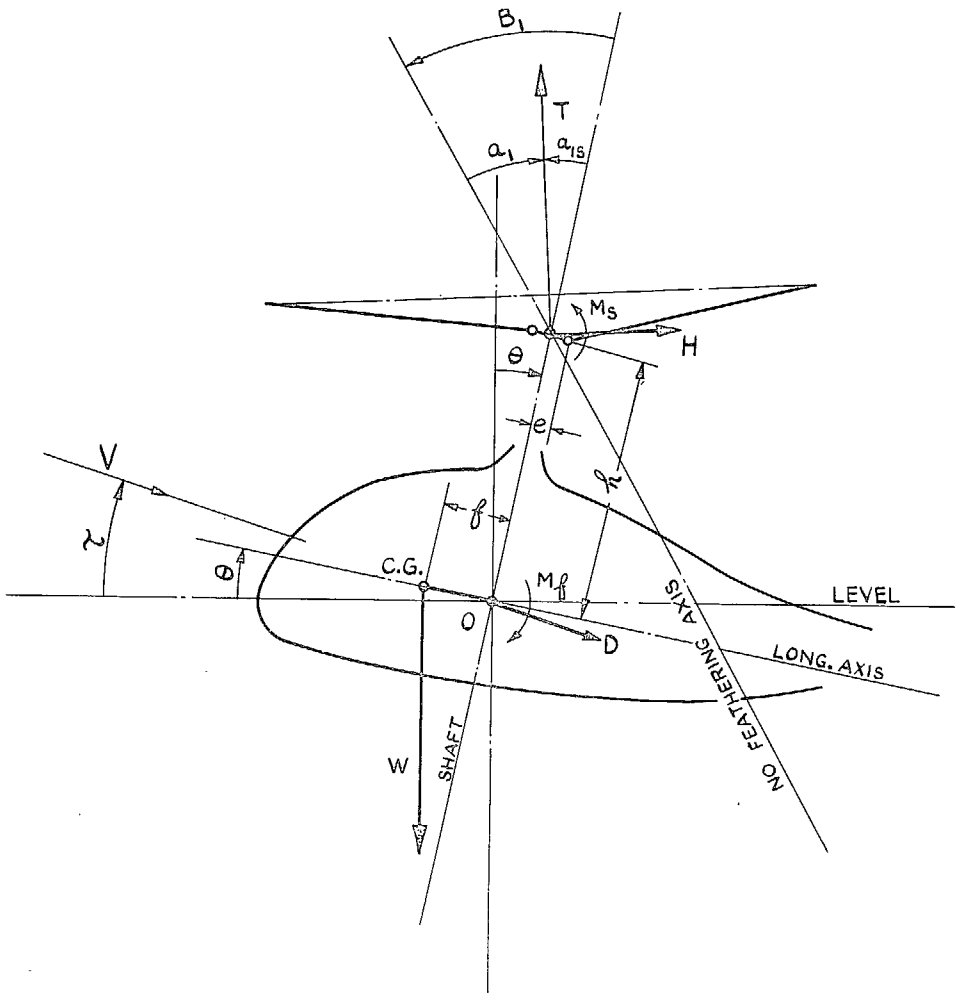

FIG. 3. Diagram for forces and moments in steady rectilinear flight.

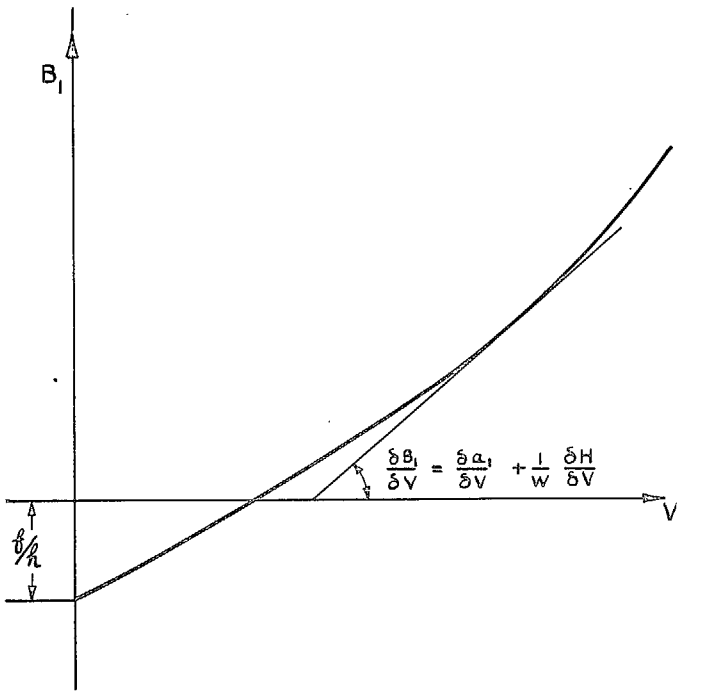

FIG. 4. Longitudinal tilt of no-feathering axis *vs.* speed.

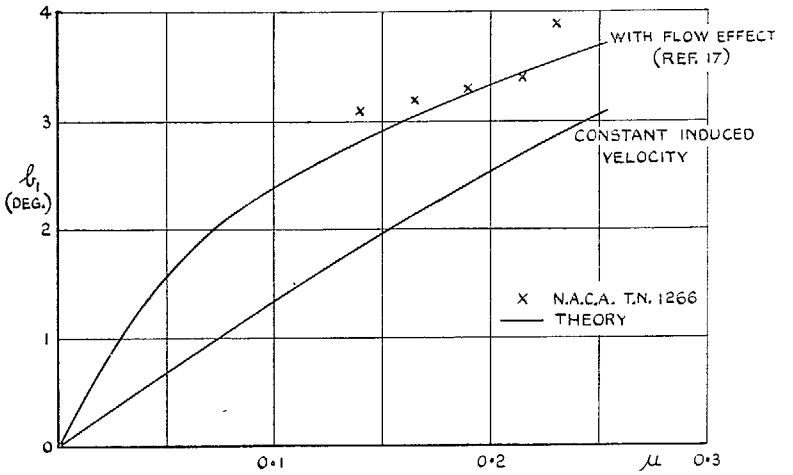

FIG. 5. Lateral flapping coefficient. R–4B helicopter.

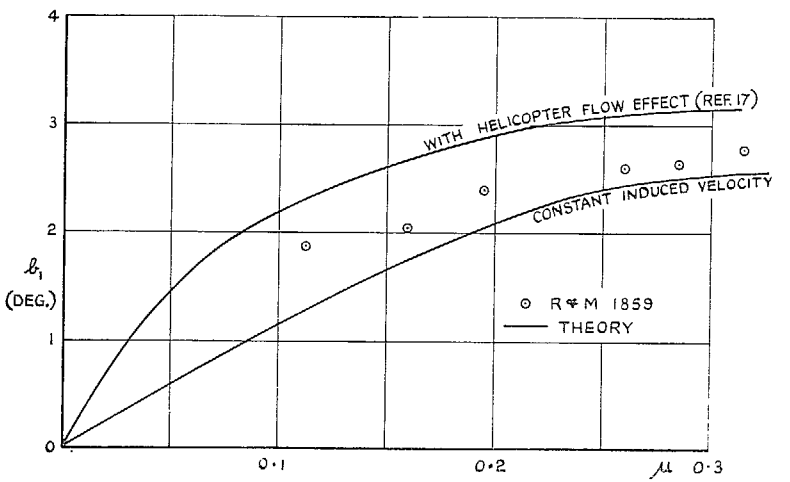

FIG. 6. Lateral flapping coefficient. C–30 autogyro.

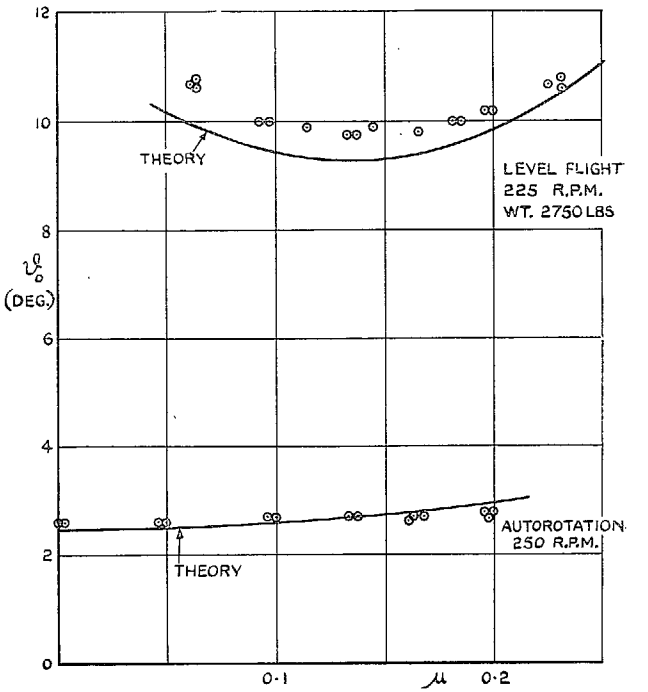

FIG. 7. Collective pitch angles. R–4B helicopter.

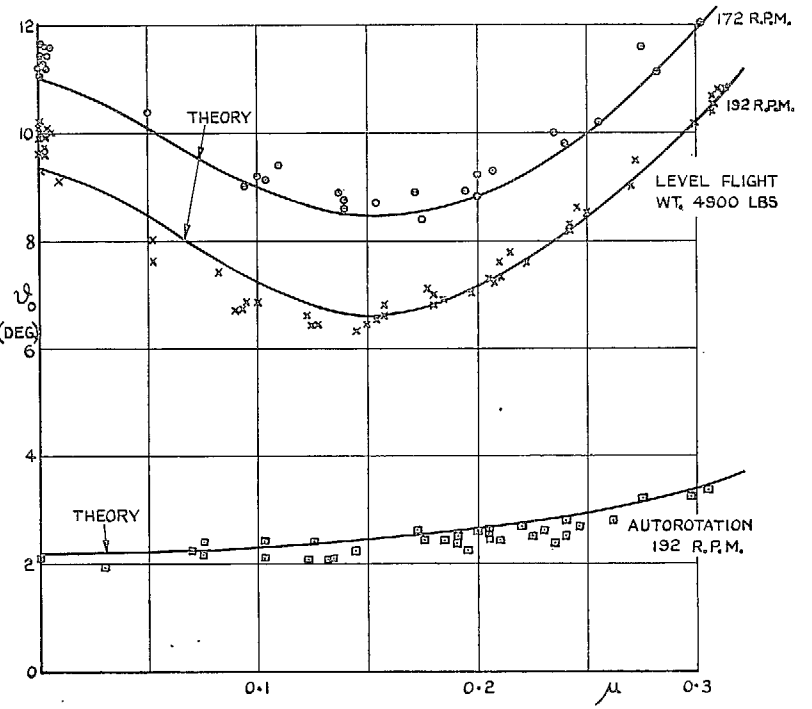

FIG. 8. Collective pitch angles. S–51 helicopter.

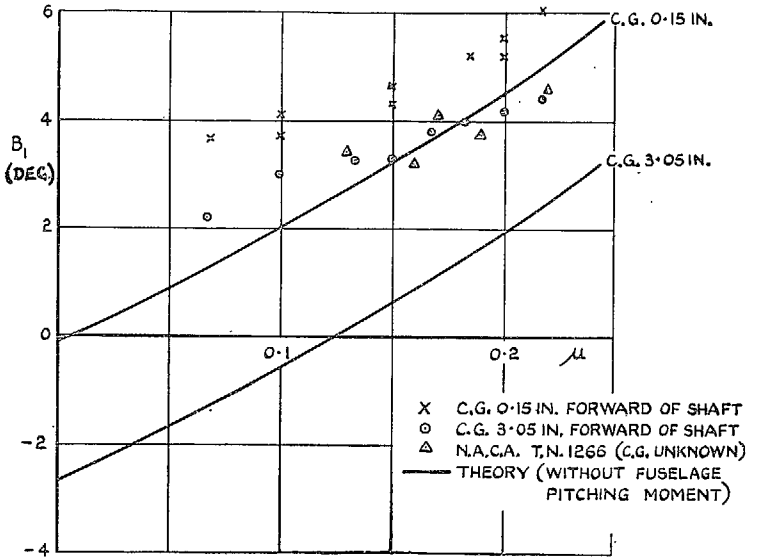

FIG. 9. Longitudinal control to trim. R–4B. Level flight.

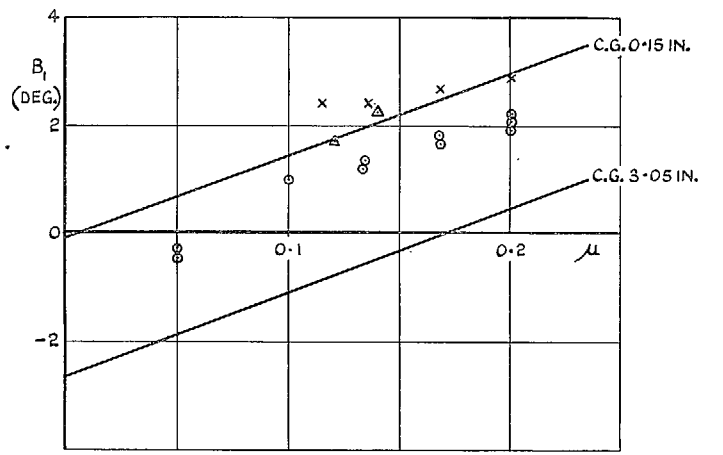

FIG. 10. Longitudingal control to trim. R–4B. Autorotation.

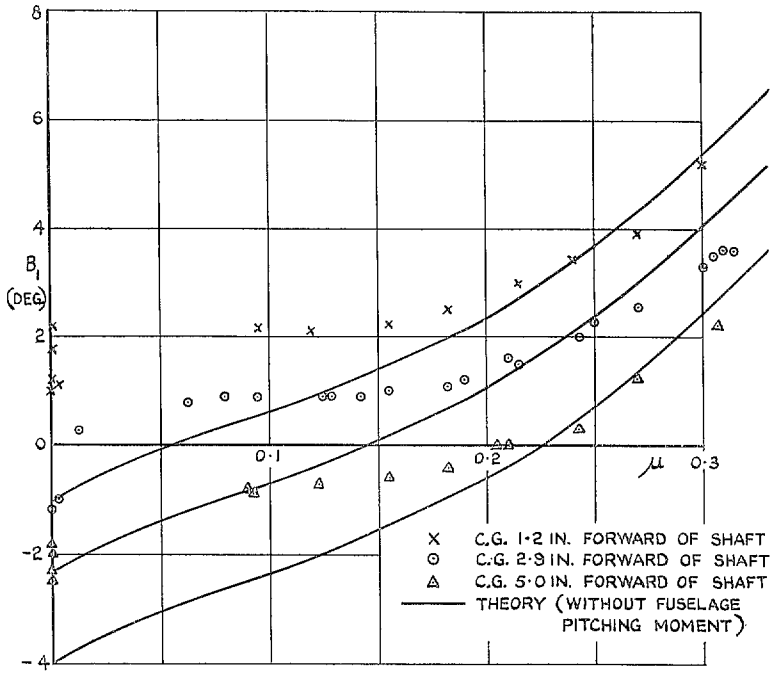

FIG. 11. Longitudinal control to trim. S–51. Level flight. 192 r.p.m.

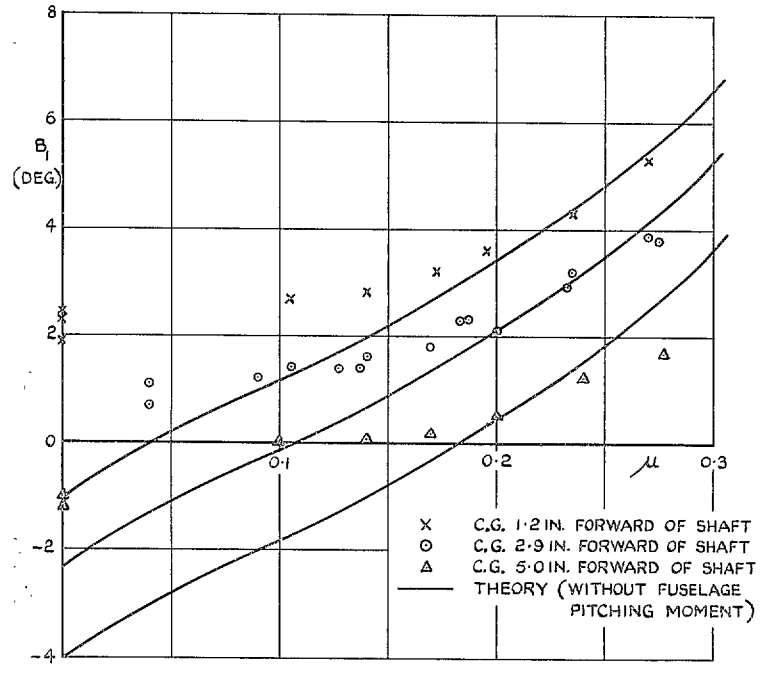

FIG. 12. Longitudinal control to trim. S–51. Level flight. 172 r.p.m.

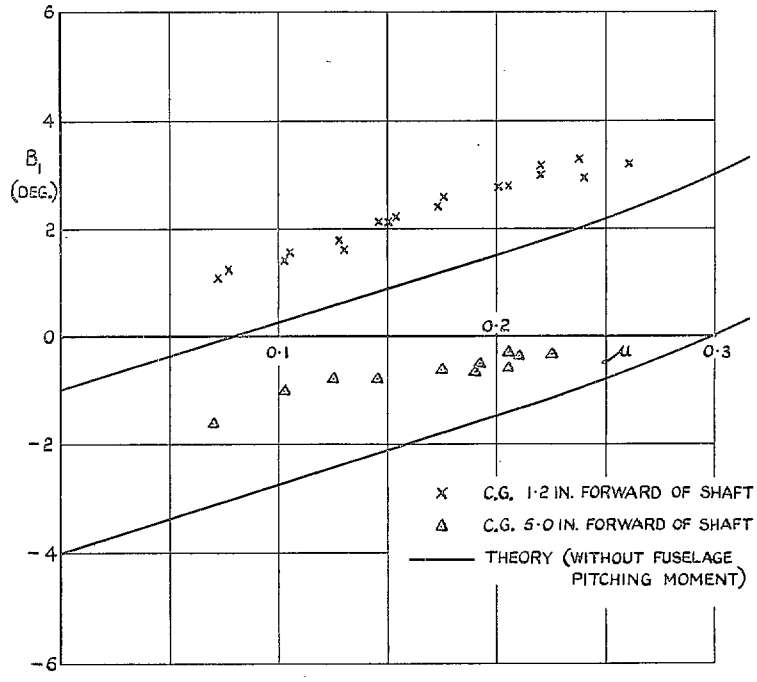

FIG. 13. Longitudinal control to trim. S–51. Autorotation. 192 r.p.m.

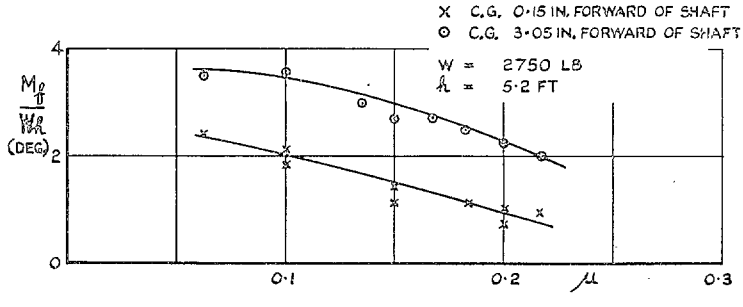

FIG. 14. Fuselage pitching moment. R–4B. Level flight.

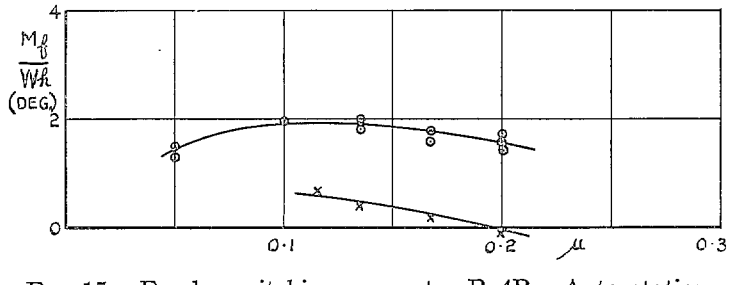

FIG. 15. Fuselage pitching moment. R–4B. Autorotation.

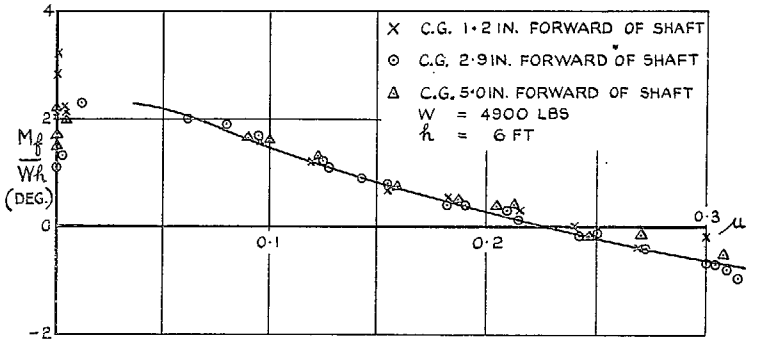

FIG. 16. Fuselage pitching moment. S–51.
Level flight. 192 r.p.m.

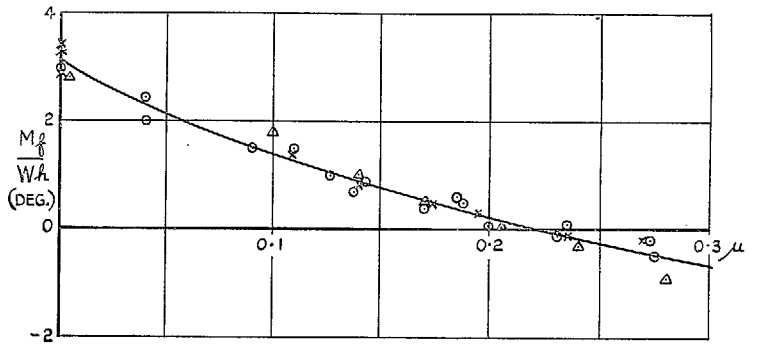

FIG. 17. Fuselage pitching moment. S–51.
Level flight. 172 r.p.m.

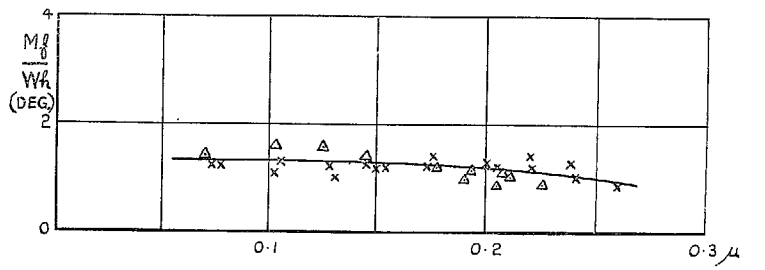

FIG. 18. Fuselage pitching moment. S–51.
Autorotation.

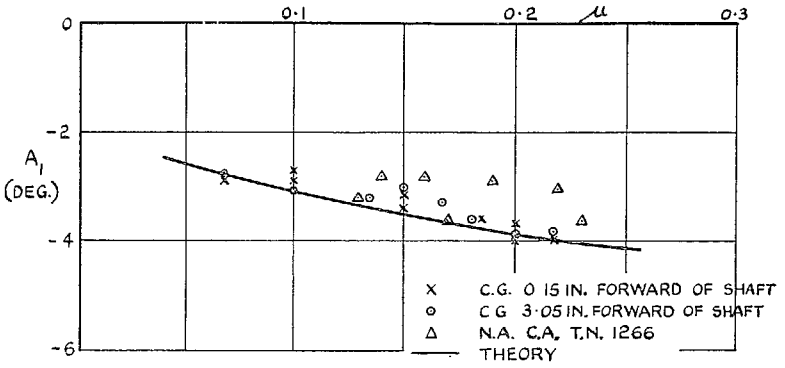

FIG. 19. Lateral control to trim. R–4B. Level flight.

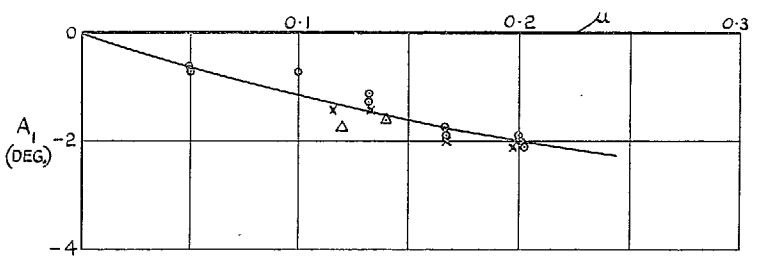

FIG. 20. Lateral control to trim. R–4B. Autorotation.

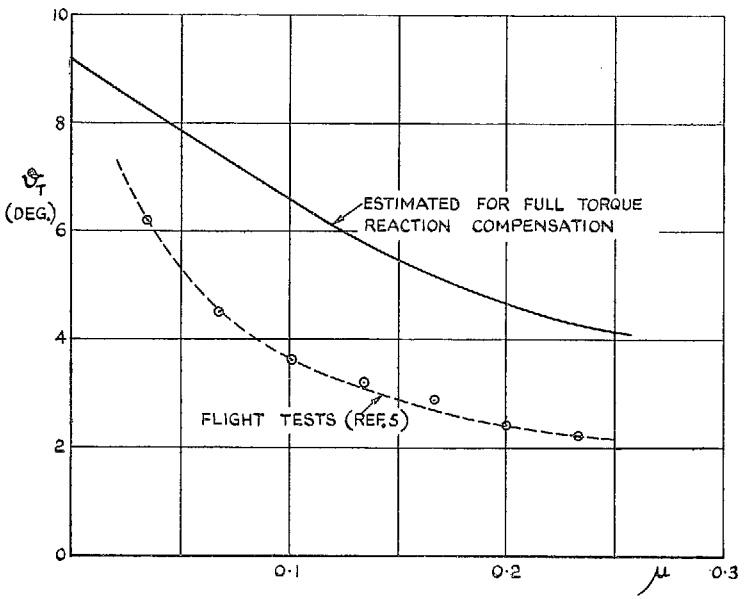

FIG. 21. Tail-rotor pitch. R–4B helicopter.

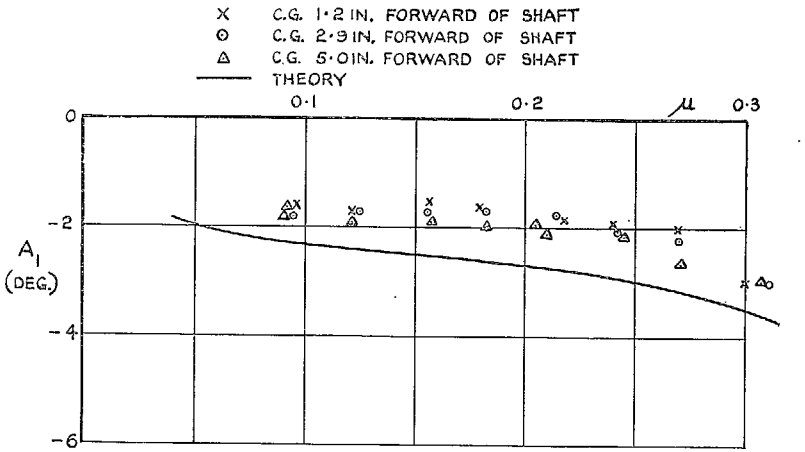

FIG. 22. Lateral control to trim. S–51. Level flight. 192 r.p.m.

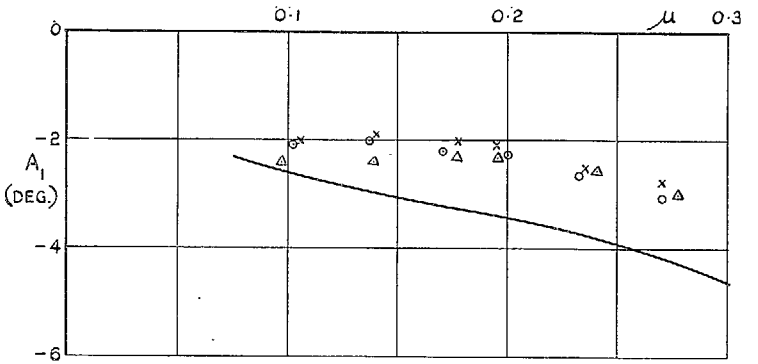

FIG. 23. Lateral control to trim. S–51. Level flight. 172 r.p.m.

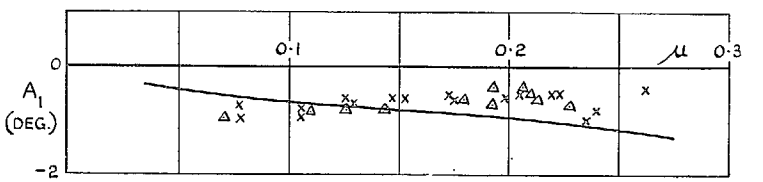

FIG. 24. Lateral control to trim. S–51. Level flight. 192 r.p.m.

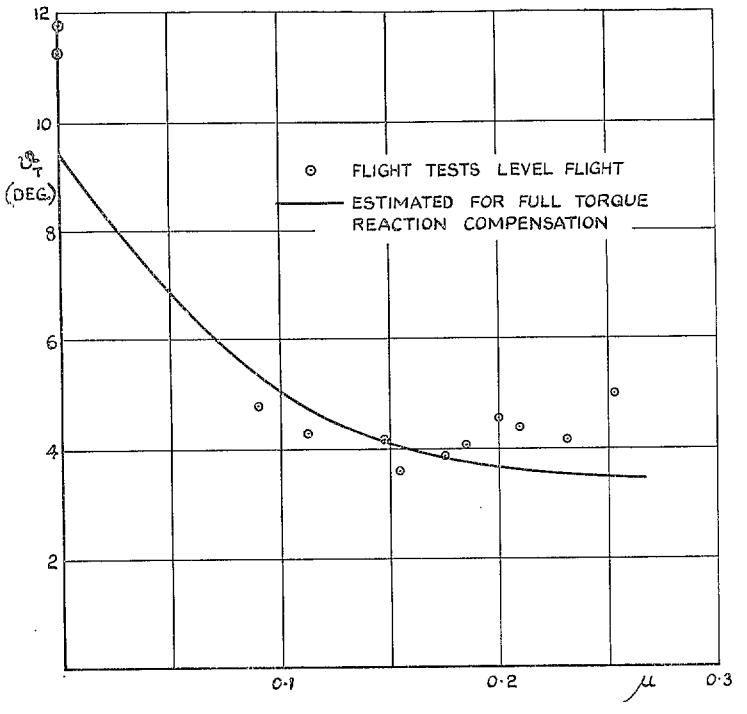

FIG. 25. Tail-rotor pitch. S–51 helicopter.

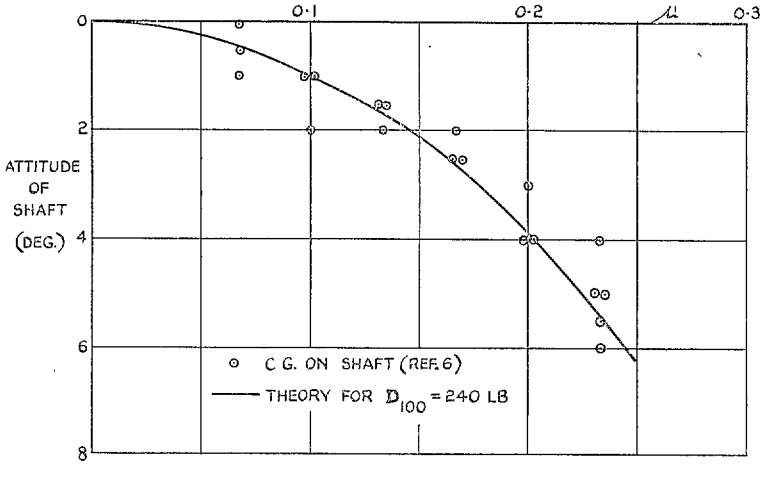

FIG. 26. Attitude of R–4B helicopter.

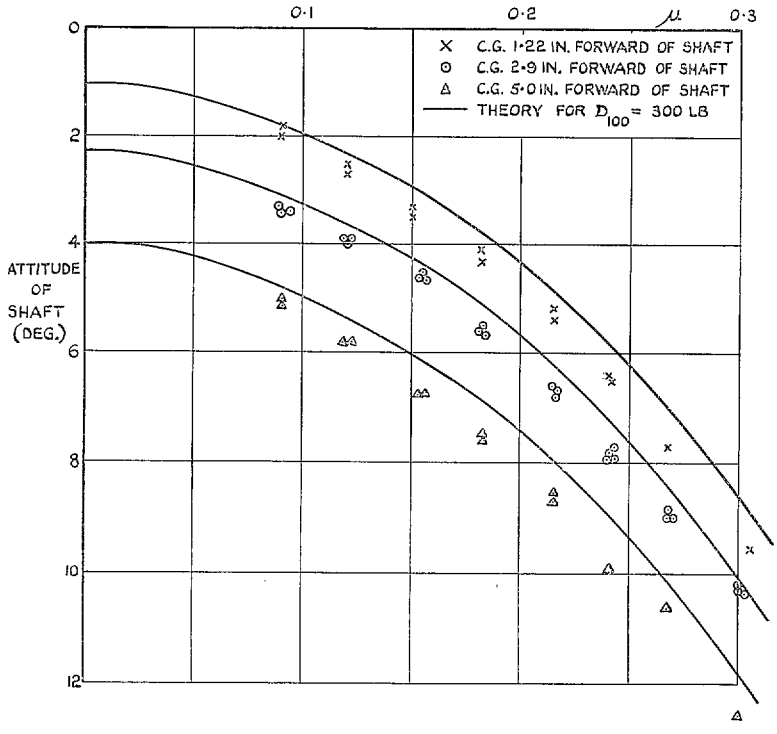

FIG. 27. Attitude of S–51 in level flight.

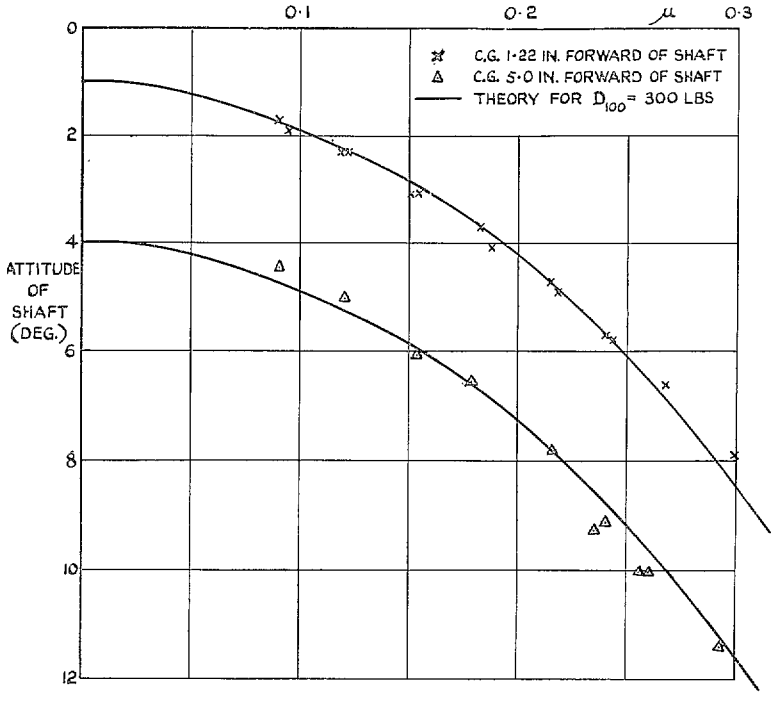

FIG. 28. Attitude of S–51 in autorotation.

(59937) Wt. 17/680 K.9. 5/54 Hw.

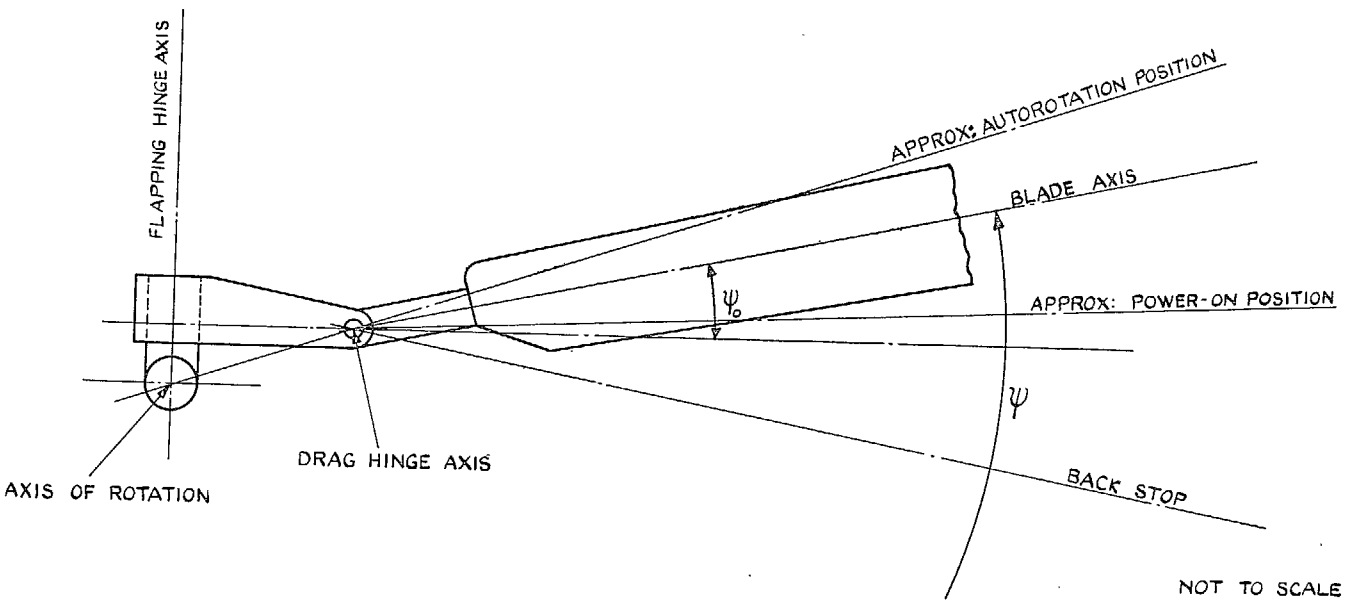

FIG. 29. S–51. Rotor-head configuration.

PRINTED IN GREAT BRITAIN

Publications of the Aeronautical Research Council

ANNUAL TECHNICAL REPORTS OF THE AERONAUTICAL RESEARCH COUNCIL (BOUND VOLUMES)

1936 Vol. I. Aerodynamics General, Performance, Airscrews, Flutter and Spinning. 40*s.* (41*s.* 1*d.*)
Vol. II. Stability and Control, Structures, Seaplanes, Engines, etc. 50*s.* (51*s.* 1*d.*)

1937 Vol. I. Aerodynamics General, Performance, Airscrews, Flutter and Spinning. 40*s.* (41*s.* 1*d.*)
Vol. II. Stability and Control, Structures, Seaplanes, Engines, etc. 60*s.* (61*s.* 1*d.*)

1938 Vol. I. Aerodynamics General, Performance, Airscrews. 50*s.* (51*s.* 1*d.*)
Vol. II. Stability and Control, Flutter, Structures, Seaplanes, Wind Tunnels, Materials. 30*s.* (31*s.* 1*d.*)

1939 Vol. I. Aerodynamics General, Performance, Airscrews, Engines. 50*s.* (51*s.* 1*d.*)
Vol. II. Stability and Control, Flutter and Vibration, Instruments, Structures, Seaplanes, etc. 63*s.* (64*s.* 2*d.*)

1940 Aero and Hydrodynamics, Aerofoils, Airscrews, Engines, Flutter, Icing, Stability and Control, Structures, and a miscellaneous section. 50*s.* (51*s.* 1*d.*)

1941 Aero and Hydrodynamics, Aerofoils, Airscrews, Engines, Flutter, Stability and Control, Structures. 63*s.* (64*s.* 2*d.*)

1942 Vol. I. Aero and Hydrodynamics, Aerofoils, Airscrews, Engines. 75*s.* (76*s.* 3*d.*)
Vol. II. Noise, Parachutes, Stability and Control, Structures, Vibration, Wind Tunnels. 47*s.* 6*d.* (48*s.* 7*d.*)

1943 Vol. I. Aerodynamics, Aerofoils, Airscrews. 80*s.* (81*s.* 4*d.*)
Vol. II. Engines, Flutter, Materials, Parachutes, Performance, Stability and Control, Structures. 90*s.* (91*s.* 6*d.*)

1944 Vol. I. Aero and Hydrodynamics, Aerofoils, Aircraft, Airscrews, Controls. 84*s.* (85*s.* 8*d.*)
Vol. II. Flutter and Vibration, Materials, Miscellaneous, Navigation, Parachutes, Performance, Plates and Panels, Stability, Structures, Test Equipment, Wind Tunnels. 84*s.* (85*s.* 8*d.*)

Annual Reports of the Aeronautical Research Council—

1933–34	1*s.* 6*d.* (1*s.* 8*d.*)	1937	2*s.* (2*s.* 2*d.*)
1934–35	1*s.* 6*d.* (1*s.* 8*d.*)	1938	1*s.* 6*d.* (1*s.* 8*d.*)
April 1, 1935 to Dec. 31, 1936	4*s.* (4*s.* 4*d.*)	1939–48	3*s.* (3*s.* 2*d.*)

Index to all Reports and Memoranda published in the Annual Technical Reports, and separately—

April, 1950 - - - - R. & M. No. 2600. 2*s.* 6*d.* (2*s.* 7½*d.*)

Author Index to all Reports and Memoranda of the Aeronautical Research Council—

1909–1949. R. & M. No. 2570. 15*s.* (15*s.* 3*d.*)

Indexes to the Technical Reports of the Aeronautical Research Council—

December 1, 1936 — June 30, 1939.	R. & M. No. 1850.	1*s.* 3*d.* (1*s.* 4½*d.*)
July 1, 1939 — June 30, 1945.	R. & M. No. 1950.	1*s.* (1*s.* 1½*d.*)
July 1, 1945 — June 30, 1946.	R. & M. No. 2050.	1*s.* (1*s.* 1½*d.*)
July 1, 1946 — December 31, 1946.	R. & M. No. 2150.	1*s.* 3*d.* (1*s.* 4½*d.*)
January 1, 1947 — June 30, 1947.	R. & M. No. 2250.	1*s.* 3*d* (1*s.* 4½*d.*)
July, 1951.	R. & M. No. 2350.	1*s.* 9*d.* (1*s.* 10½*d.*)

Prices in brackets include postage.

Obtainable from

HER MAJESTY'S STATIONERY OFFICE

York House, Kingsway, London, W.C.2; 423 Oxford Street, London, W.1 (Post Orders: P.O. Box 569, London, S.E.1); 13a Castle Street, Edinburgh 2; 39, King Street, Manchester 2; 2 Edmund Street, Birmingham 3; 1 St. Andrew's Crescent, Cardiff; Tower Lane, Bristol 1; 80 Chichester Street, Belfast, or through any bookseller

S.O. Code No. 23–2733